2234 *Organometallics* **2010,** *29,* 2234–2247
DOI: 10.1021/om900970x

ORGANOMETALLICS
Article

Toward Supramolecular Assembly of 10-Vertex {*closo*-2,1,10-FeC_2B_7} Clusters: Intramolecular Imidate Formation and Polymetallic, Polycluster Species

Andreas Franken, Thomas D. McGrath,* and F. Gordon A. Stone

Department of Chemistry & Biochemistry, Baylor University, Waco, Texas 76798-7348

Received November 5, 2009

Addition of Me_3NO to CH_2Cl_2 solutions of [1-OH-2,2,2-$(CO)_3$-*closo*-2,1,10-$FeC_2B_7H_8$] (**1a**) affords [2,2-$(CO)_2$-1,2-μ-{OCH_2NMe_2}-*closo*-2,1,10-$FeC_2B_7H_8$] (**2**), which contains a five-membered FeNCOC unit. The same reaction in MeCN as solvent gives [2,2-$(CO)_2$-1,2-μ-{OC(R)NH}-*closo*-2,1,10-$FeC_2B_7H_8$] (**3a**, R = Me). Analogous derivatives [R = CH═C(H)Me (**3c**), *p*-$C_6H_4NO_2$ (**3d**), *p*-C_6H_4Br (**3f**), *p*-$C_6H_4C(H)O$ (**3g**), *p*-$C_6H_4C{\equiv}CH$ (**3h**), *p*-C_5H_4N (**3i**), or NH_2 (**3j**)] are obtained from treatment of CH_2Cl_2 solutions of **1a** with other cyano-containing substrates and Me_3NO. The μ-imidate species **3** undergo a variety of subsequent reactions. Thus, oxidative coupling of compound **3h** in CH_2Cl_2, in the presence of CuCl−TMEDA (TMEDA = $Me_2NCH_2CH_2NMe_2$), affords dimeric [2,2-$(CO)_2$-*closo*-2,1,10-$FeC_2B_7H_8$-1,2-μ-{$OC(N^{Fe}H)$-*p*-C_6H_4-C≡C}]$_2$ (**4**), which reacts with [$Co_2(CO)_8$] in CH_2Cl_2 to give the tetracluster species [2,2-$(CO)_2$-*closo*-2,1,10-$FeC_2B_7H_8$-1,2-μ-{$OC(N^{Fe}H)$-*p*-C_6H_4-{(μ-η^2:η^2-C≡C)$Co_2(CO)_6$}}]$_2$ (**5**). Conversely, **3f** forms a bis(cluster) species, [2,2′-dppb-{2-CO-1,2-μ-{$OC(C_6H_4Br)NH$}-*closo*-2,1,10-$FeC_2B_7H_8$}$_2$] (**6**), upon reaction with dppb (0.5 mol equiv) in refluxing THF (dppb = $Ph_2P(CH_2)_4PPh_2$; THF = tetrahydrofuran). Compound **3a** in CH_2Cl_2 with $PHPh_2$ and Me_3NO yields [2-CO-2-$PHPh_2$-1,2-μ-{OC(Me)NH}-*closo*-2,1,10-$FeC_2B_7H_8$] (**7**), which, upon reaction with wet NEt_3 in CH_2Cl_2, gives [$NHEt_3$][2-CO-2-{$P(O)Ph_2$}-1,2-μ-{OC(Me)NH}-*closo*-2,1,10-$FeC_2B_7H_8$] (**8**). When a mixture of C_6H_6−CH_2I_2 was used in the latter reaction, the product was [2-CO-2-$PIPh_2$-1,2-μ-{OC(Me)NH}-*closo*-2,1,10-$FeC_2B_7H_8$] (**9**), which itself reacts with AgO_2CMe, forming [2-CO-2-{$P(O_2CMe)Ph_2$}-1,2-μ-{OC(Me)NH}-*closo*-2,1,10-$FeC_2B_7H_8$] (**10**). Compound **3a** reacts with excess [NBu^n_4]CN in CH_2Cl_2 to form the anionic complex [1-OH-2,2-$(CO)_2$-2-CN-*closo*-2,1,10-$FeC_2B_7H_8$]$^-$, isolated as its [$N(PPh_3)_2$]$^+$ salt (**11**), in which the intramolecular imidate portion of the precursor has been lost. The anion of **11** readily coordinates via the cyano group to the cationic {$Ir(CO)(PPh_3)_2$}$^+$ fragment (formed from [$IrCl(CO)(PPh_3)_2$] and $TlPF_6$), affording [2-{(μ-CN)$Ir(CO)(PPh_3)_2$}-1-OH-2,2-$(CO)_2$-*closo*-2,1,10-$FeC_2B_7H_8$] (**12**). Oxidative addition of MeI to the Ir(I) center in **12** gives the corresponding Ir(III) species [2-{(μ-CN)Ir(I)(Me)$(CO)(PPh_3)_2$}-1-OH-2,2-$(CO)_2$-*closo*-2,1,10-$FeC_2B_7H_8$] (**13**). The novel structural features of these compounds—including hydrogen-bonding interactions—were confirmed by single-crystal X-ray diffraction studies.

Introduction

The polyhedral boranes and their derivatives have fascinated and challenged chemists since Stock's discovery of the first polyboron hydrides over a century ago.[1] Although in some ways they have been viewed as scientific curiosities, many boron-containing clusters have found applications by virtue of their unique properties.[2] At present much research focuses on functionalization of these clusters,[2b,c] with many potential applications envisaged in diverse areas: from materials science[3] to cancer chemotherapy,[2c,4] from treatment of nuclear waste[5] to enzyme inhibition,[6] and ion sensing.[7] All these applications depend upon the preparation of molecules with precisely tailored properties, and thus the development of a range of substrates and a battery of routes for their

*To whom correspondence should be addressed. E-mail: tom_mcgrath@baylor.edu.

(1) Stock, A. *Hydrides of Boron and Silicon*; Cornell Univ. Press: Ithaca, NY, 1933.

(2) See, together with references therein: (a) Plešek, J. *Chem. Rev.* **1992**, *92*, 269. (b) Teixidor, F., Ed. Recent Advances in Boron Chemistry. *J. Organomet. Chem.* **2009**, *694*, 1587. (c) Hawthorne, M. F. *Chem. Eng. News* **2009**, *87*, 16.

(3) For example: (a) Masalles, C.; Llop, J.; Viñas, C.; Teixidor, F. *Adv. Mater.* **2002**, *14*, 826. (b) Gentil, S.; Crespo, E.; Rojo, I.; Friang, A.; Viñas, C.; Teixidor, F.; Grüner, B.; Gabel, D. *Polymer* **2005**, *46*, 12218. (c) Mola, J.; Mas-Marza, E.; Sala, X.; Romero, I.; Rodríguez, M.; Viñas, C.; Parella, T.; Llobet, A. *Angew. Chem., Int. Ed.* **2008**, *47*, 5830. (d) Nieuwenhuyzen, M.; Seddon, K. R.; Teixidor, F.; Puga, A. V.; Viñas, C. *Inorg. Chem.* **2009**, *48*, 889.

(4) Hawthorne, M. F. *Angew. Chem., Int. Ed.* **1993**, *32*, 950. Valliant, J. F.; Guenther, K. J.; King, A. S.; Morel, P.; Schaffer, P.; Sogbein, O. O.; Stephenson, K. A. *Coord. Chem. Rev.* **2002**, *232*, 173.

(5) Viñas, C.; Gomez, S.; Bertran, J.; Teixidor, F.; Dozol, J.-F.; Rouquette, H. *Inorg. Chem.* **1998**, *37*, 3640. Clark, J. F.; Chamberlin, R. M.; Abney, K. D.; Strauss, S. H. *Environ. Sci. Technol.* **1999**, *33*, 2489.

(6) Cígler, P.; Kožíšek, M.; Řezáčová, P.; Brynda, J.; Otwinowski, Z.; Pokorná, J.; Plešek, J.; Grüner, B.; Dolečková-Marešová, L.; Máša, M.; Sedláček, J.; Bodem, J.; Kräusslich, H.; Král, V.; Konvalinka, J. *Proc. Natl. Acad. Sci. U. S. A.* **2005**, *102*, 15394.

(7) Stoica, A.-I.; Viñas, C.; Teixidor, F. *Chem. Commun.* **2009**, 4988.

 Published on Web 04/21/2010

Chart 1

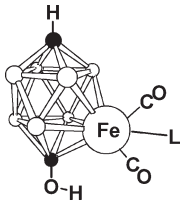

L

1a	CO
1b	PEt_3
1c	NMe_3*
1d	NCMe*

(* – not isolated)

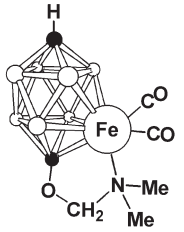

2

OBH ●C

functionalization is important in facilitating the study of these compounds' potential.

While investigating the reaction of the eight-vertex monocarborane $[closo\text{-}1\text{-}CB_7H_8]^-$ with iron carbonyls, we unexpectedly discovered a straightforward synthesis of the iron–dicarbollide complex [1-(OH)-2,2,2-$(CO)_3$-*closo*-2,1,10-$FeC_2B_7H_8$] (**1a**; see Chart 1), along with its anionic manganese analogue from a corresponding reaction with $[Mn_2(CO)_{10}]$.[8] As these compounds bear a terminal hydroxyl substituent, they were attractive candidates for further reactivity studies, and we have reported the results of reactions that form a variety of derivatives of both the iron[9] and manganese[10] species. In seeking to expand the derivative chemistry of the former system, fortuitous discoveries have led us to several compounds containing intramolecular $\overline{\text{FeNCOC}}$ rings, as we here elaborate. Some aspects of this work have been communicated.[11]

Results and Discussion

Formation of Intramolecular $\overline{\text{FeNCOC}}$ Rings. We have recently reported the synthesis[8,9] of the iron–dicarbollide complex [1-OH-2,2,2-$(CO)_3$-*closo*-2,1,10-$FeC_2B_7H_8$] (**1a**) in a process that involves insertion of both an $\{Fe(CO)_3\}$ fragment *and* an additional CO moiety (both from $[Fe_2(CO)_9]$) into the monocarborane cluster $[closo\text{-}1\text{-}CB_7H_8]^-$. In addition to CO substitution at the metal center, giving species such as [1-OH-2,2-$(CO)_2$-2-PEt_3-*closo*-2,1,10-$FeC_2B_7H_8$] (**1b**), compound **1a** also undergoes a variety of reactions that involve further functionalization through reactions at the cage-bound hydroxyl group.[9] As part of a program to extend all aspects of this chemistry, we repeated the reaction forming **1b**,[8,9] but omitted the added PEt_3. Thus, treatment of **1a** in CH_2Cl_2 with Me_3NO alone was expected to produce the species [1-OH-2,2-$(CO)_2$-2-NMe_3-*closo*-2,1,10-$FeC_2B_7H_8$] (**1c**), in which a CO ligand of the precursor is lost as CO_2 and the remaining NMe_3 molecule coordinates to the metal center. Such a species could be a useful synthon for further studies of reactivity at the Fe center. However, the product instead formed is the compound [2,2-$(CO)_2$-1,2-μ-$\{OCH_2NMe_2\}$-*closo*-2,1,10-$FeC_2B_7H_8$] (**2**), which contains a five-membered $\overline{\text{FeNCOC}}$ intramolecular ring. (A propensity for ring formation in 10-vertex ferracarboranes has been noted in derivatives of **1a**[9] and in a related $\{FeCB_8\}$ cluster.[12])

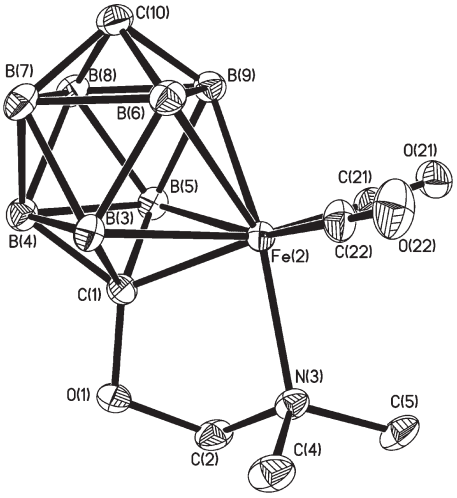

Figure 1. Structure of **2** showing the crystallographic labeling scheme. In this and Figures 7–11, thermal ellipsoids are shown with 40% probability, and for clarity (where relevant) only chemically significant H atoms are shown. Selected distances (Å) and angles (deg): C(1)–O(1) 1.403(3), C(1)–Fe(2) 1.937(2), O(1)–C(2) 1.406(3), C(2)–N(3) 1.483(3), N(3)–Fe(2) 2.0943(18), O(1)–C(1)–Fe(2) 117.08(15), C(1)–O(1)–C(2) 108.53(16), O(1)–C(2)–N(3) 107.98(17), C(2)–N(3)–Fe(2) 103.75(13), C(1)–Fe(2)–N(3) 79.43(8).

The details of the structure of **2** were revealed by an X-ray diffraction study (Figure 1): its architecture may be viewed as being derived from **1c** via loss of H_2, with one H atom each coming from N-CH_2H and cage-O*H* groups. An O atom from the Me_3NO reagent might also be involved, so that overall (at least formally) H_2O is eliminated in the process (rather than H_2). In any case, assuming **1c** to be the initially formed product, it is neither unprecedented nor wholly unexpected for C–H activation to take place in such species where a molecule of eliminated NMe_3 becomes coordinated to the metal center.[12,13] Metal-mediated hydrogen loss from

(8) Franken, A.; Lei, P.; McGrath, T. D.; Stone, F. G. A. *Chem. Commun.* **2006**, 3423.
(9) Franken, A.; McGrath, T. D.; Stone, F. G. A. *Organometallics* **2008**, *27*, 908.
(10) Franken, A.; McGrath, T. D.; Stone, F. G. A. *Organometallics* **2009**, *28*, 225.
(11) Franken, A.; McGrath, T. D.; Stone, F. G. A. *Dalton Trans.* **2009**, 7353.
(12) Franken, A.; Hodson, B. E.; McGrath, T. D.; Stone, F. G. A. *Inorg. Chem.* **2008**, *47*, 8788.
(13) See also, for example: Johnson, B. F. G.; Lewis, J.; Pearsall, M.-A.; Scott, L. G. *J. Organomet. Chem.* **1991**, *402*, C27. Mathur, P.; Singh, A. K.; Mohanty, J. R.; Chatterjee, S.; Mobin, S. M. *Organometallics* **2008**, *27*, 5094.

Table 1. ^{1}H, ^{13}C, and ^{11}B NMR Data[a]

compd	$^{1}H/\delta$[b]	$^{13}C/\delta$[c]	$^{11}B/\delta$[d]
2	5.74 (br s, 1H, cage CH), 4.72 (s, 2H, CH_2), 2.97 (s, 6H, 2 × CH_3)	211.7 (CO), 198.3 (br, cage CO), 98.4 (CH_2), 70.8 (br, cage CH), 52.3 (CH_3)	−0.8, −12.1 (2B), −19.6 (4B)
3a[e]	7.50 (br s, 1H, cage CH), 5.81 (br s, 1H, NH), 2.64 (s, 3H, CH_3)	210.4 (CO), 191.0 (br, cage CO), 181.9 (C═N), 70.4 (br, cage CH)	−3.0, −12.6 (2B), −19.3 (2B), −20.6 (2B)
3c	7.42 (br s, 1H, cage CH), 7.10 (br s, 1H, ═CH), 6.23 [d, *J*(HH) = 13, 1H, ═CH], 5.82 (br s, 1H, NH), 2.10 (s, 3H, CH_3)	210.4 (CO), 191.5 (br cage CO), 178.3 (C═N), 145.5 (═CH), 117.7 (═*C*HMe), 70.1 (br, cage CH), 18.2 (CH_3)	−2.9, −12.6 (2B), −19.3 (2B), −20.5 (2B)
3d	8.63 (br s, 1H, cage CH), 8.49−7.95 (m, 4H, C_6H_4), 5.94 (br s, 1H, NH)	210.0 (CO), 190.7 (br, cage CO), 176.4 (C═N), 133.5−124.2 (C_6H_4), 71.2 (br, cage CH)	−2.3, −12.3 (2B), −19.1 (2B), −20.4 (2B)
3e	7.84−6.84 (m, 4H, C_6H_4), 7.62 (br s, 1H, cage CH), 5.82 (br s, 1H, NH), 4.40 (s, 2H, NH_2)	210.8 (CO), 191.8 (br, cage CO), 179.5 (C═N), 151.1−114.2 (C_6H_4), 69.8 (br, cage CH)	−3.0, −12.6 (2B), −19.4 (2B), −20.3 (2B)
3f	8.38 (br s, 1H, cage CH), 7.93−7.59 (m, 4H, C_6H_4), 5.89 (br s, 1H, NH)	210.3 (CO), 181.9 (br, cage CO), 178.2 (C═N), 133.5−125.5 (C_6H_4), 70.6 (br, cage CH)	−2.6, −12.4 (2B), −19.2 (2B), −20.4 (2B)
3g	10.13 (s, 1H, CHO), 8.24 (br s, 1H, cage CH), 8.03−7.53 (m, 4H, C_6H_4), 5.89 (br s, 1H, NH),	210.4 (CO), 190.7 (CHO), 185.0 (br, cage CO), 177.7 (C═N), 132.9−127.0 (C_6H_4), 70.9 (br, cage CH)	−2.6, −12.4 (2B), −19.2 (2B), −20.4 (2B)
3h[e]	8.24 (br s, 1H, cage CH), 8.01−7.76 (m, 4H, C_6H_4), 5.89 (br s, 1H, NH), 3.46 (s, 1H, ≡CH)	210.3 (CO), 191.1 (br, cage CO), 177.9 (C═N), 132.9−125.5 (C_6H_4), 81.9 (C*C*≡), 81.4 (≡CH), 70.6 (br, cage CH)	−2.6, −12.4 (2B), −19.2 (2B), −20.4 (2B)
3i	8.97−7.54 (m, 5H, C_5H_4N and cage CH), 5.86 (br s, 1H, NH)	212.4 (CO), 187.5 (br, cage CO), 176.3 (C═N), 151.5−150.1 (C_5H_4N), 71.4 (br, cage CH)	−2.4, −12.3 (2B), −19.0 (2B), −20.5 (2B)
3j	5.79 (br s, 1H, NH), 5.38 (br s, 2H, NH_2), 5.00 (br s, 1H, cage CH)	211.1 (CO), 187.0 (br, cage CO), 167.9 (C═N), 70.7 (br, cage CH)	−3.3, −12.5 (2B), −19.7 (4B)
4[e]	8.24 (br s, 2H, cage CH), 8.04−7.72 (m, 8H, C_6H_4), 5.90 (br s, 2H, NH)	210.0 (CO), 184.0 (br, cage CO), 177.7 (C═N), 133.0−125.5 (C_6H_4), 81.6, 76.8 (≡C), 70.5 (br, cage CH)	−2.5, −12.4 (2B), −19.1 (2B), −20.3 (2B)
5[e]	8.25 (br s, 2H, cage CH), 8.08−7.78 (m, 8H, C_6H_4), 5.91 (br s, 2H, NH)	210.3 (Fe-CO), 196.2 (Co-CO), 184.0 (br, cage CO), 178.1 (C═N), 145.3−124.6 (C_6H_4), 96.4, 92.5 (C_2Co_2), 70.6 (br, cage CH)	−2.5, −12.4 (2B), −19.2 (2B), −20.3 (2B)
6	7.68−7.32 (m, 28H, Ph and C_6H_4), 6.83 (br s, 2H, cage CH), 5.79 (br s, 2H, NH), 2.56 (br, 4H, PCH_2), 2.29 (br, 4H, PCH_2CH_2)	217.0 [d, *J*(PC) = 32, CO], 182.3 (br, cage CO), 175.9 (C═N), 134.2−124.8 (Ph and C_6H_4), 64.0 (br, cage CH), 30.2 [d, *J*(PC) = 25, PCH_2], 26.5 (PCH_2CH_2)	−0.7, −12.1 (2B), −19.5 (2B), −22.4 (2B)
7	7.76 (br s, 1H, cage CH), 7.49−7.18 (m, 10H, Ph), 6.52 [d, *J*(PH) = 376, 1H, PH], 6.21 (br s, 1H, NH), 2.42 (s, 3H, CH_3)	216.7 [d, *J*(PC) = 35, CO], 190.4 (br, cage CO), 179.4 (C═N), 133.6−128.0 (Ph), 64.1 (br, cage CH), 18.7 (CH_3)	−6.2, −11.2,−14.9, −19.2, −20.5 (2B), −22.7
8	7.47−7.21 (m, 10H, Ph), 6.22 (br s, 1H, cage CH), 5.72 (br s, 1H, NH), 4.57 (br, 1H, N*H*Et_3), 3.76 (m, 6H, CH_2), 2.44 (s, 3H, CH_3), 1.87 (m, 9H, CH_3)	216.0 [d, *J*(PC) = 37, CO], 189.8 (br, cage CO), 180.0 (C═N), 134.7−127.6 (Ph), 68.0 (NCH_2), 65.0 (br, cage CH), 25.8 (NCH_2-*C*H_3), 19.1 (*C*H_3)	−7.6, −12.0, −15.3, −19.1, −20.2 (2B), −23.5
9	7.45−7.14 (m, 10H, Ph), 6.24 (br s, 1H, cage CH), 5.83 (br s, 1H, NH), 2.78 (s, 3H, CH_3)	214.7 [d, *J*(PC) = 38, CO], 191.3 (br, cage CO), 179.8 (C═N), 134.6−128.8 (Ph), 63.4 (br, cage CH), 19.2 (CH_3)	−6.6, −11.9, −14.7, −19.4, −20.2 (2B), −21.9
10	7.93 (br s, 1H, cage CH), 7.62−7.48 (m, 10H, Ph), 5.29 (br s, 1H, NH), 2.60 (s, 3H, CH_3), 2.23 (s, 3H, CH_3)	215.6 [d, *J*(PC) = 37, CO], 187.2 (br, cage CO), 179.9 (C═N), 169.9 (POC═O), 132.5−127.9 (Ph), 67.7 (CH_3), 22.6 (br, cage CH), 18.9 (CH_3)	−4.4, −7.5, −15.5, −16.2, −19.0, −21.8, −23.6
11	7.65−7.48 (m, 30H, Ph), 6.33 (br s, 1H, cage CH), 3.78 (br s, 1H, cage COH)	211.9 (CO), 183.4 (br, cage CO), 145.1 (C≡N), 133.8−126.5 (Ph), 76.8 (br, cage CH)	5.9, −3.4 (2B), −17.3 (2B), −23.2 (2B)
12	7.75−7.49 (m, 30H, Ph), 5.75 (br s, 1H, cage CH), 3.79 (br s, 1H, cage COH)	208.8 (CO), 183.6 (br, cage CO), 166.0 [t, *J*(PC) = 23, Ir−CO], 146.3 (C≡N), 134.4−128.4 (Ph), 79.0 (br, cage CH)	8.8, −2.0 (2B), −17.8 (2B), −23.2 (2B)
13	7.90−7.29 (m, 30H, Ph), 5.93 (br s, 1H, cage CH), 3.53 (br s, 1H, cage COH), 1.60 (s, 3H, CH_3)	20.9.1 (CO), 185.0 (br, cage CO), 174.7 [t, *J*(PC) = 30, Ir−CO], 144.8 (C≡N), 134.7−128.7 (Ph), 66.3 (br, cage CH), 15.3 (CH_3)	9.4, −1.7 (2B), −17.2 (2B), −22.9 (2B)

[a] Chemical shifts (δ) in ppm, coupling constants (*J*) in hertz, measurements at ambient temperatures in CD_2Cl_2. [b] Resonances for terminal BH protons occur as broad unresolved signals in the range δ ca. −3 to +3. [c] ^{1}H-decoupled chemical shifts are positive to high frequency of $SiMe_4$. [d] ^{1}H-decoupled chemical shifts are positive to high frequency of $BF_3 \cdot Et_2O$ (external); resonances are of unit integral except where indicated. [e] Data from ref 10.

Me_2N−hydrocarbyl groups has also been implicated in other systems.[14] Although the precise mechanism is not entirely clear in the present reaction, we have eliminated the possibility that the CH_2Cl_2 solvent is the source of the O−*C*H_2−N methylene group in **2** by repeating the reaction in, for example, CD_2Cl_2, $PhCHCl_2$, and THF (tetrahydrofuran) as solvents: in each case, **2** was the only metallacarborane isolated and always in comparable yields. The five-membered ring in **2** is puckered into an envelope conformation, so that C(2) lies about 0.63 Å above the {C(1)Fe(2)N(3)O(1)} plane; the {C(1)Fe(2)N(3)O(1)}−{O(1)C(2)N(3)} interplane angle is 47.7(2)°. Although the molecule lacks crystallographic symmetry, molecular mirror symmetry is evident in its NMR spectra (Table 1), with the $^{11}B\{^{1}H\}$ NMR spectrum revealing a 1:2:4 (2+2 coincidence) pattern of resonances, while both ^{1}H and $^{13}C\{^{1}H\}$ NMR spectra indicate the two Me groups likewise to be equivalent on the NMR time scale. In solution at ambient temperature, therefore, the {O(1)C(2)N(3)} "flap" of the envelope is flipping between the two faces of the {C(1)Fe(2)-N(3)O(1)} plane.

(14) For example: Hitchcock, P. B.; Handley, D. A.; Lee, T. H.; Leigh, G. J. *J. Chem. Soc., Dalton Trans.* **2002**, 4720.

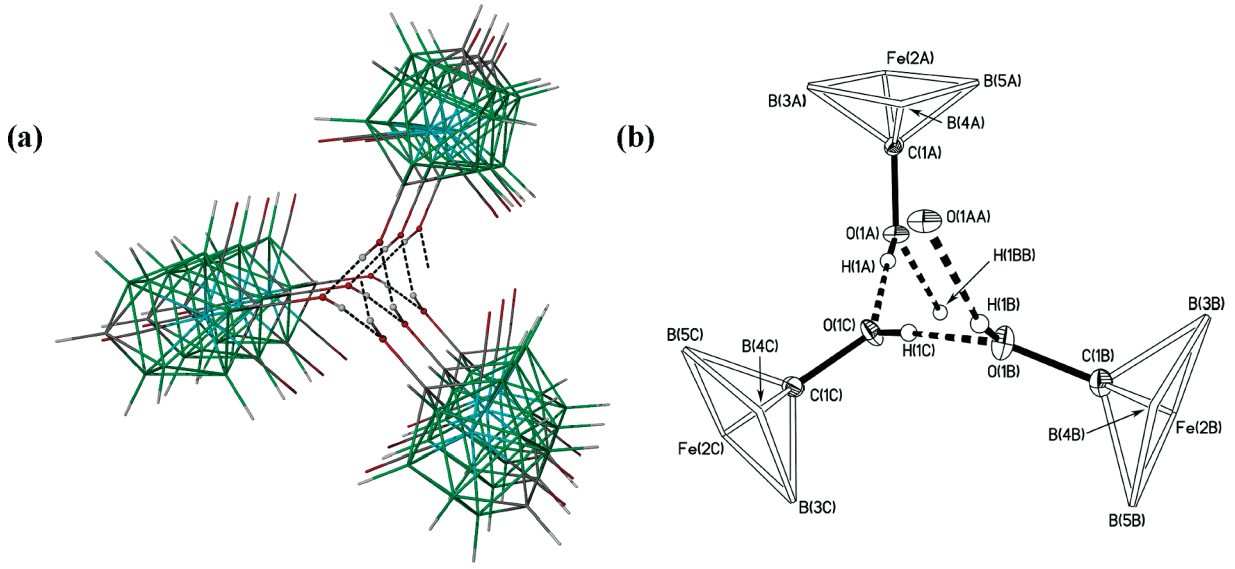

Figure 2. (a) Representation of one of the hydrogen-bonded helices of compound **1a** in its crystals. In this and in Figures 3−6, atoms are color-coded as follows: boron, green; iron, light blue; carbon, gray; hydrogen, white; nitrogen, dark blue; oxygen, red. (b) Detail of the hydrogen bonding in a single "turn" of the helix, looking along *a* toward the *bc* plane. The atom labels of the three independent molecules have two characters in parentheses, ending ...A, ...B, or ...C. The atom O(1AA) has coordinates $x+1$, y, z relative to O(1A) with x, y, z, and the atom H(1BB) has coordinates $x-1$, y, z relative to H(1B) with x, y, z. Selected distances (Å) and angles (deg): O(1A)−H(1A), O(1B)−H(1B), and O(1C)−H(1C) were fixed at 0.84; H(1A)···O(1C) 2.11, O(1A)···O(1C) 2.949(3), O(1A)−H(1A)···O(1C) 177.2; H(1B)···O(1AA) 2.30, O(1B)···O(1AA) 3.117(3), O(1B)−H(1B)···O(1AA) 165.5; H(1C)···O(1B) 2.20, O(1C)···O(1B) 3.036(3), O(1C)−H(1C)···O(1B) 174.1.

When the reaction forming **2** was repeated in MeCN as solvent, in the hope of forming [1-OH-2,2-$(CO)_2$-2-NCMe-*closo*-2,1,10-$FeC_2B_7H_8$] (**1d**) as a possibly more stable analogue of **1c**, we again found that the presumed initial product had reacted further. In this case, the product was [2,2-$(CO)_2$-1,2-μ-{OC(Me)NH}-*closo*-2,1,10-$FeC_2B_7H_8$] (**3a**; Chart 2), in which the Fe-bound NCMe ligand and the C(cage)-bound OH group have coupled to form an imidate (imino ester).[15,16] The process resembles the Pinner reaction,[15,17] but in this case base catalysis[18] seems more likely, with NMe_3 and/or OH^- (from traces of H_2O) the probable catalysts. Like **2**, complex **3a** contains an intramolecular five-membered FeNCOC ring, but now this ring is close to planar, a constraint imposed by the C=N double bond. The structure of **3a** was confirmed by X-ray diffraction analysis.[11]

Analogues of **3a** were prepared by treatment of CH_2Cl_2 solutions of **1a** with nitriles in the presence of Me_3NO. Thus, reactions using a variety of substrates RCN gave the corresponding imidate products [2,2-$(CO)_2$-1,2-μ-{OC(R)NH}-*closo*-2,1,10-$FeC_2B_7H_8$] [R = CH=C(H)Me (**3c**), *p*-$C_6H_4NO_2$ (**3d**), *p*-C_6H_4Br (**3f**), *p*-$C_6H_4C(H)O$ (**3g**), *p*-$C_6H_4C{\equiv}CH$ (**3h**), *p*-C_5H_4N (**3i**), or NH_2 (**3j**)], with the exception of **3c**, which was prepared from $CH_2{=}CHCH_2CN$, with the allyl group in the expected product (**3b**) undergoing an internal rearrangement in the course of the reaction. The latter fact was confirmed by NMR data and by an X-ray diffraction study, the results of which are included as Supporting Information. An additional derivative [R = *p*-$C_6H_4NH_2$ (**3e**)] was obtained from **3d** by straightforward borohydride reduction ($NaBH_4$−EtOH) of its nitro group.

Chart 2

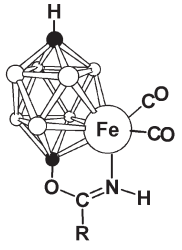

R

3a Me
3b $CH_2CH{=}CH_2$ *
3c $CH{=}CHCH_3$
3d 4-$C_6H_4NO_2$
3e 4-$C_6H_4NH_2$
3f 4-C_6H_4Br
3g 4-$C_6H_4C(H)O$
3h 4-$C_6H_4C{\equiv}CH$
3i 4-C_5H_4N
3j NH_2

(* − not isolated)

○BH ●C

All of compounds **3** have broadly similar NMR spectroscopic properties (Table 1), except for characteristic peaks due to the various substituents R. Thus, all nine compounds show almost identical $^{11}B\{^1H\}$ NMR spectra, with 1:2:2:2 intensity patterns showing retention of molecular mirror symmetry on the NMR time scale. In their ^1H NMR spectra, the imine NH proton appears as a broad signal around δ

(15) Roger, R.; Neilson, D. G. *Chem. Rev.* **1961**, *61*, 179.
(16) Recent reviews include: Michelin, R. A.; Mozzon, M.; Bertani, R. *Coord. Chem. Rev.* **1996**, *147*, 299. Kukushkin, V. Yu.; Pombeiro, A. J. L. *Chem. Rev.* **2002**, *102*, 1771.
(17) Pinner, A.; Klein, F. *Berichte* **1877**, *10*, 1889.
(18) Schaefer, F. C.; Peters, G. A. *J. Org. Chem.* **1961**, *26*, 412.

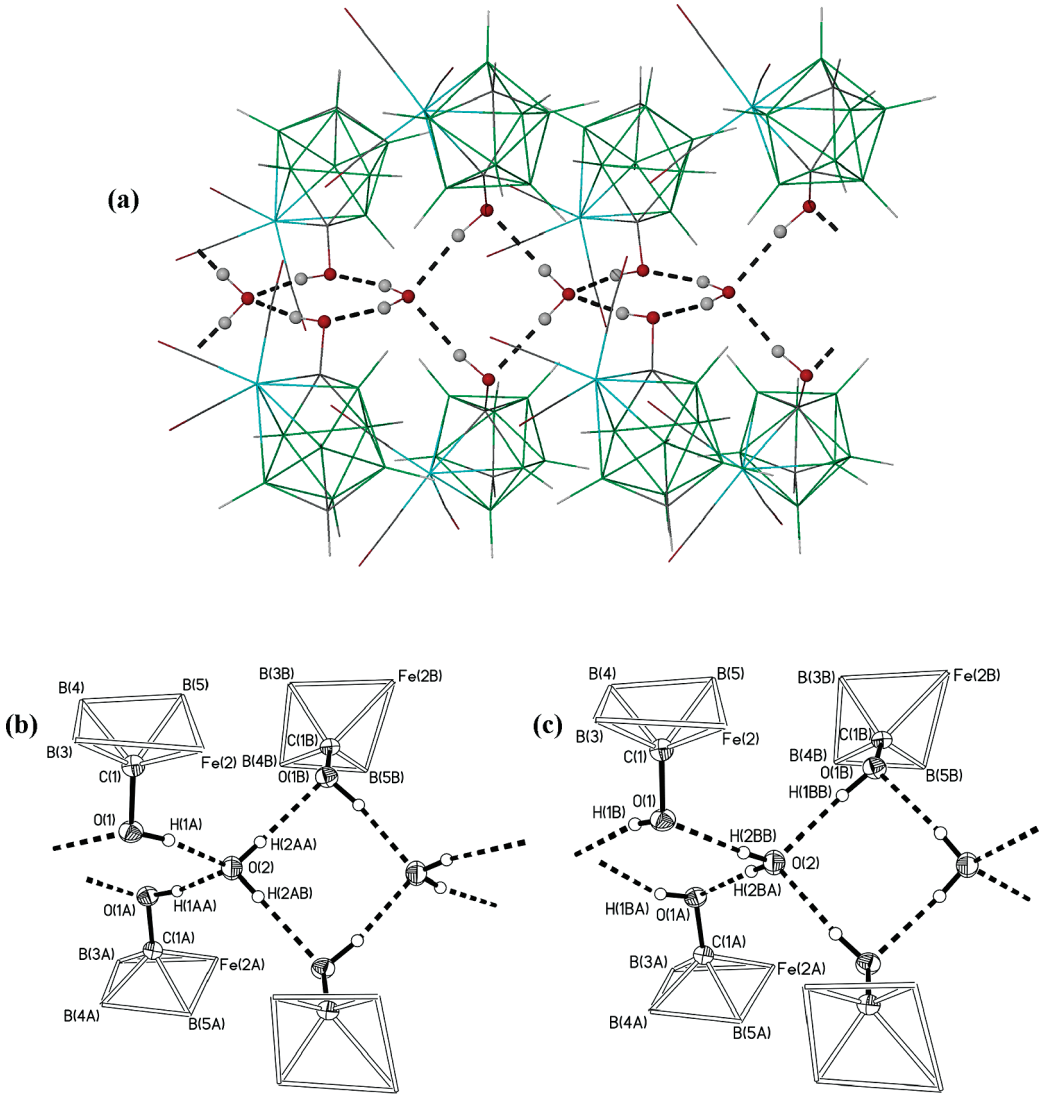

Figure 3. (a) Representation of one of the types of hydrogen bonding in crystals of **1a**·H_2O. (b) Detail of the hydrogen-bonding interactions in (a). In this and in (c) the atom C(1A) has coordinates $^3/_2 - x$, $^1/_2 - y$, z, and the atom C(1B) has coordinates $^1/_2 + y$, $1 - x$, $^1/_2 + z$, relative to C(1) with coordinates x, y, z, and so on. Selected distances (Å) and angles (deg): O(1)−H(1A) 0.8726(15), H(1A)···O(2) 1.8522(16), O(1)···O(2) 2.713(2), O(1)−H(1A)···O(2) 168.53(11); O(2)−H(2AA) 0.82(3), H(2AA)···O(1B) 1.93(3), O(2)···O(1B) 2.736(2), O(2)−H(2AA)···O(1B) 171(5). (c) Alternative mode of hydrogen bonding in **1a**·H_2O. Selected distances and angles: O(2)−H(2BB) 0.81(3), H(2BB)···O(1) 1.91(3), O(2)···O(1) 2.713(2), O(2)−H(2BB)···O(1) 173(5); O(1B)−H(1BB) 0.8300(15), H(1BB)···O(2) 1.9291(16), O(1B)···O(2) 2.736(2), O(1B)−H(1BB)···O(2) 163.75(11).

5.8−5.9, while in the $^{13}C\{^1H\}$ NMR spectra, the two distinct types of cluster-carbon vertices resonate around δ 190 (cage CO) and 70 (cage CH), as is to be expected, and the imidate C═N carbon atoms are seen around δ 170−180. This reaction between an activated, Fe-bound nitrile and the adjacent hydroxyl oxygen atom appears to be quite versatile and tolerant of a range of functional groups. In addition to the derivatives noted above, several other cyano compounds react similarly with compound **1a**, evidently giving products analogous to compounds **3** (as judged by characteristic signals in NMR spectra), but isolation of these species in sufficiently pure form proved difficult.[19]

Hydrogen Bonding and Structural Chemistry in Crystals of Compounds 1a and 3. In our initial report[8] upon the formation of compounds **1a** and **1b**, it was noted that crystals of **1b** contain two crystallographically independent molecules that form weakly hydrogen-bonded pairs. Moreover, molecules of the ruthenium analogue of compound **1a** crystallize such that they form hydrogen-bonded helices that extend throughout the crystal.[7] It was of interest, therefore, to look for similar behavior in crystals of compound **1a**, and also in several of the compounds **3**, that contain the imidate N−H as a possible donor and various heteroatoms as potential acceptors.

Crystals of compound **1a** were isomorphous with those of its ruthenium analogue so that there are again three crystallographically independent molecules in the asymmetric fraction of the unit cell that combine to form one "turn" of a helix that extends along the crystallographic a direction. These are represented in Figure 2. (As the molecules crystallize in the centrosymmetric space group $P\bar{1}$, there is another set of opposite handed helices in the opposite a direction.)

(19) Such problems are further highlighted by the observation that compound **3f** can remain associated with one equivalent of *p*-BrC_6H_4CN, to the extent that the two compounds *cocrystallize*; this determination is included as Supporting Information.

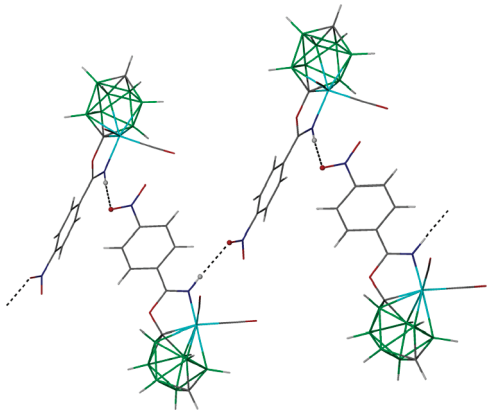

Figure 4. Four hydrogen-bonded molecules of compound **3d** in the solid state. These zigzag chains extend in the crystallographic *a* direction, each molecule generated from the previous one by $^3/_2 - x$, $^1/_2 + y$, $^3/_2 - z$. The N−H distance was fixed at 0.88 Å, H···O is 2.17 Å, N···O is 3.045(3) Å, and N−H···O is 176.3°.

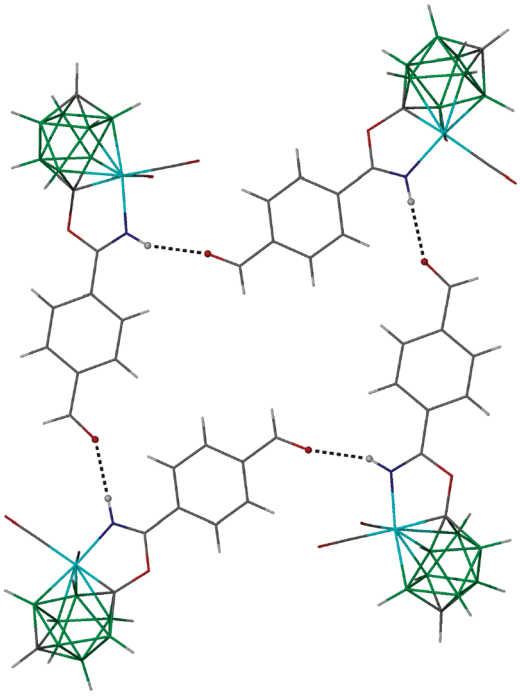

Figure 5. Four hydrogen-bonded molecules of compound **3g** in the solid state. Two adjacent molecules constitute the asymmetric portion of the unit cell, with the other generated by symmetry operation $-x$, $-y$, $-1-z$. The N−H distance was fixed at 0.88 Å, and one type of N−H···O hydrogen bond has parameters H···O 2.09 Å, N···O 2.967(2) Å, and N−H···O 173.4°; the other has H···O 2.11 Å, N···O 2.940(2) Å, and N−H···O 157.5°.

The donor···acceptor (O···O) distances are close to 3 Å, so the O−H···O interactions are relatively weak,[20] but nevertheless they are evidently sufficient to produce the observed packing in the solid state.

A second crystalline form of compound **1a**, as its 1:1 H_2O solvate, was also analyzed and found to have much stronger[20] hydrogen-bonding interactions between the hydroxyl O−H of **1a** and the solvate molecule. These are illustrated in Figure 3 and can be seen to consist of alternating molecules of **1a** and H_2O, arranged along a 4_2 axis in the crystallographic *c* direction (space group $P4_2/n$). Some disorder is evident, with two alternative positions for the C(cage)−hydroxyl hydrogen, which may be compared in Figure 3 (b and c), so that in any given $(\mathbf{1a}\cdot H_2O)_n$ "chain" only one set of orientations is possible.

Of the various different compounds **3** with potential heteroatom acceptors for hydrogen bonding, only **3d** (Figure 4), **3g** (Figure 5), and **3i** (Figure 6) displayed any such interactions in the solid state. In all three cases, the interactions are rather weak, as judged by the donor··· acceptor distances all being around 3 Å, but, as was the case with compound **1a**, they are evidently sufficient to direct the observed packing of these molecules in the crystalline state. It is notable that the arrangement of molecules in the solid state is different in each case and seemingly is dictated by the geometry of the imidate substituent R relative to the N−H vector of the imine portion. Thus, for example, in **3i**, the angle between the axis of the pyridyl ring and the imine N−H bond is approximately 120°, leading to the 3-fold type of symmetry observed. Perhaps surprisingly no significant hydrogen bonding was observed in crystals of **3e** and **3j**.

Reactivity of Compounds Containing Intramolecular FeNCOC Rings: Polycluster Derivatives. Taking compounds **3** as a starting point, it was of interest so see if these versatile building blocks could form the basis for synthesizing larger, supramolecular complexes. Two initial strategies that might lead to bis(cage) compounds presented themselves, namely, (a) linking two $\{FeC_2B_7\}$ clusters by a bis(imidate) species (route **A** → **B** in Scheme 1) and (b) linking two $\{FeC_2B_7\}$ clusters via a bidentate ligand, so that the product contains a Fe−L⁓L′−Fe′ bridge (route **A** → **C** in Scheme 1). Both of these approaches have led to polycluster compounds, as we now illustrate.

Terminal alkynes such as that in compound **3h** may be coupled in the presence of Cu(I) salts to give diacetylenes.[21] Thus, **3h** was treated in CH_2Cl_2 with CuCl−TMEDA (TMEDA = $Me_2NCH_2CH_2NMe_2$), with aerobic oxidation, to give a dimeric species, [2,2-$(CO)_2$-*closo*-2,1,10-$FeC_2B_7H_8$-1,2-μ-{OC(N^{Fe}H)-*p*-C_6H_4-C≡C}]$_2$ (**4**; see Chart 3).[11] A single molecule of **4** is rather anisotropic, being approximately 28 Å (estimated) along the molecular axis, versus only around 6 Å in the orthogonal direction.[11] The two alkyne functions in compound **4** can themselves react with $[Co_2(CO)_8]$ to form $\{C_2Co_2\}$ tetrahedra, a reaction that has been known for more than half a century.[22] In the case of **4**, this reaction with the cobalt reagent produced the *tetra*cluster, hexametallic species [2,2-$(CO)_2$-*closo*-2,1,10-$FeC_2B_7H_8$-1,2-μ-{OC(N^{Fe}H)-*p*-C_6H_4-{(μ-η^2:η^2-C≡C)$Co_2(CO)_6$}}]$_2$ (**5**), in which two $\{FeC_2B_7\}$ clusters are linked to a pair of $\{C_2Co_2\}$ tetrahedra.[11] The latter species was characterized crystallographically and has an approximately "V-shaped" structure in the solid state, with the two "halves" of the molecule *cisoid* with respect to the central C−C bond (crystallographic C_2 symmetry). Both **4** and **5** display all of the expected spectroscopic properties in their IR and NMR data. Attempts to form further "aggregates" of compound **4**

(20) (a) Gilli, P.; Bertolasi, V.; Ferretti, V.; Gilli, G. *J. Am. Chem. Soc.* **1994**, *116*, 909. (b) Gilli, G.; Gilli, P. *J. Mol. Struct.* **2000**, *552*, 1. (c) Steiner, T. *Angew. Chem., Int. Ed.* **2002**, *41*, 49.

(21) Hay, A. S. *J. Org. Chem.* **1960**, *25*, 1275.

(22) Pfeffer, M.; Grellier, M. In *Comprehensive Organometallic Chemistry III*; Crabtree, R. H., Mingos, D. M. P., Eds.; Pergamon Press: Oxford, U.K., 2007; Vol. 7, Chapter 7.01, and references therein.

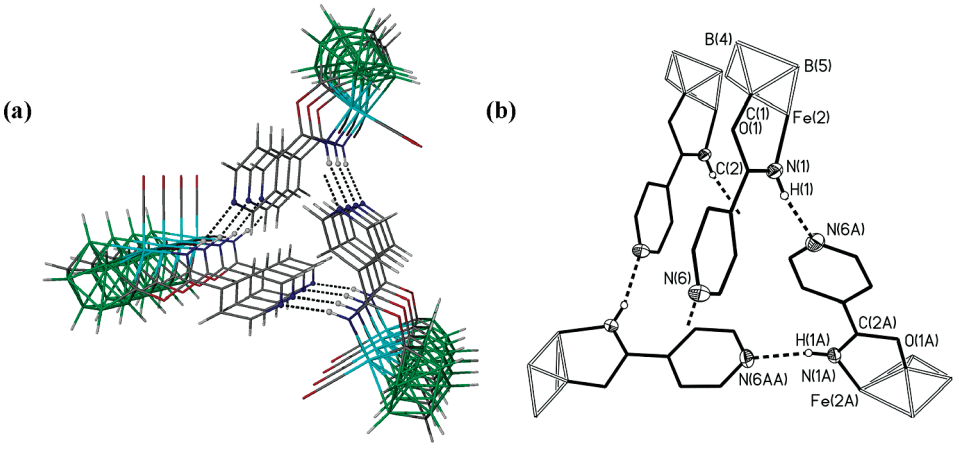

Figure 6. (a) Hydrogen-bonded helices in crystals of compound **3i**. Each molecule is generated from the previous one by $^2/_3 - y$, $^1/_3 + x - y$, $^1/_3 + z$. (b) Detail of the hydrogen bonding in a single "turn" of the helix. Selected distances (Å) and angle (deg): N(1)−H(A) 0.84(3), H(1)···N(6A) 2.10(3), N(1)···N(6A) 2.911(3), N(1)−H(1)···N(6A) 163(2).

Scheme 1. Possible Routes for Assembling Supramolecular Structures, Starting from Compounds 3 (schematic A)[a]

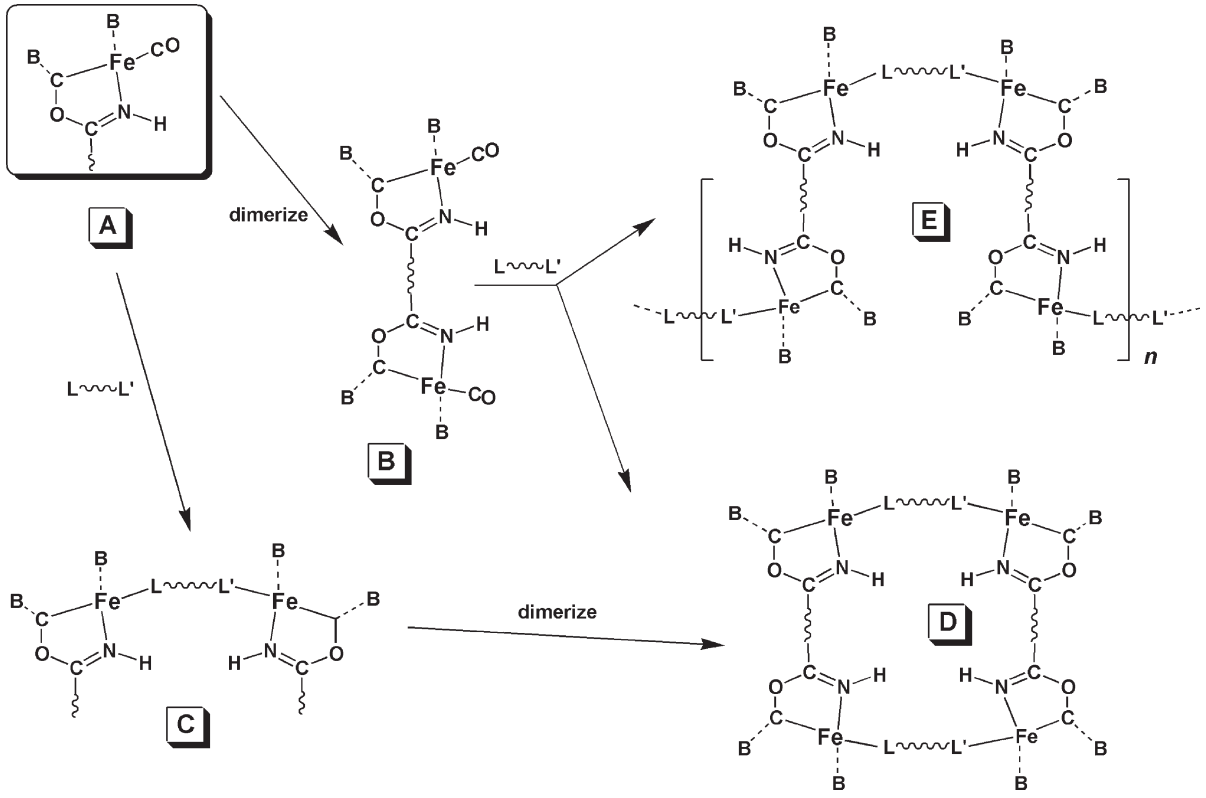

[a] ~~ is a nonspecific linker group, so that L~~L′ represents a bidentate ligand. Schematic structures **B** and **C** are exemplified by compounds **4** and **6**, respectively. For each molecule, much of the metallacarborane cluster and other Fe-bound ligands are omitted.

by linking two molecules via a bidentate ligand have thus far been frustrated by poor solubility of the presumed tetracluster product (structure "**D**" in Scheme 1), although the product mixture is so intractable that oligomeric or polymeric species (structure "**E**" in Scheme 1) cannot be excluded.

As an alternative to forming dimeric **4** from **3h**, attempts were also made to link two molecules of an imidate species **3** via bidentate ligands (route **A** → **C** in Scheme 1). Compound **3f** was chosen as a starting substrate, so that the product would retain a bromo substituent as a site for possible later dimerization (**C** → **D** in Scheme 1), and dppb [Ph_2P-$(CH_2)_4PPh_2$] was used as the bidentate ligand, this being selected to minimize steric interactions between two Fe centers and to limit the possibility of the diphosphine chelating a single metal center. Thus reaction of **3f** with dppb (2:1 molar ratio) in refluxing THF afforded the diphosphine-bridged, bis(cluster) species [2,2′-dppb-{2-CO-1,2-μ-{OC-(C_6H_4Br)NH}-*closo*-2,1,10-$FeC_2B_7H_8$}$_2$] (**6**; Chart 4).

In the solid state (Figure 7), molecules of **6** have a crystallographically imposed inversion center and retain the imidate portion of the starting compound, confirming that a CO ligand was preferentially replaced at the Fe center rather than the Fe−N(imidate) linkage being "lifted off". In its various NMR spectra, **6** displays all the expected features for

Chart 3

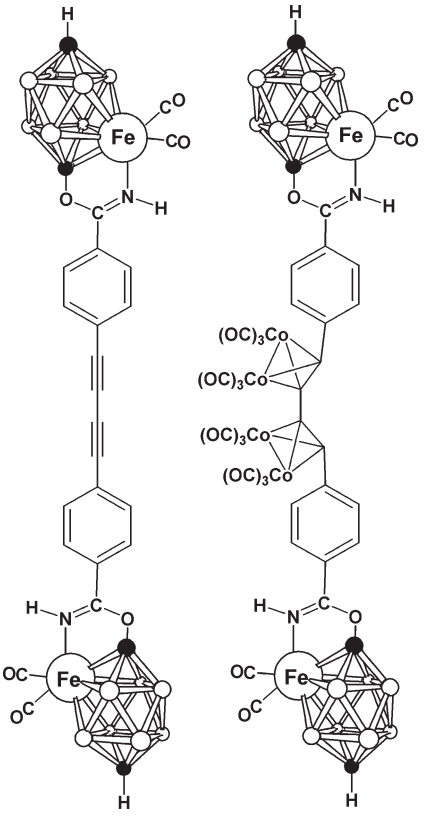

Chart 4

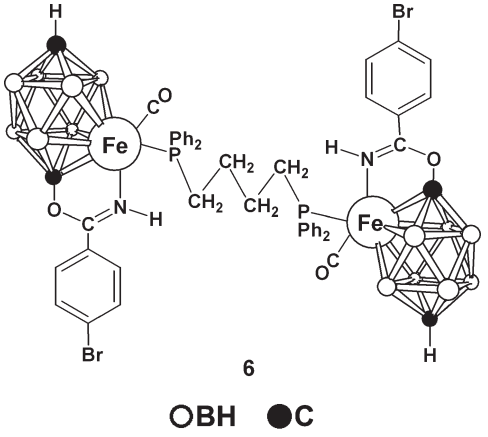

the cage, imidate, phosphine, and substituents, with loss of molecular mirror symmetry also evident. Unfortunately, however, compound **6** resisted all our attempts to form a tractable supramolecular species (route **C** → **D** in Scheme 1), but we are continuing to pursue this possibility using these and related synthetic approaches.

Reactivity of Compounds Containing Intramolecular FeNCOC Rings: Substitution at Iron. Noting that **3f** reacts with phosphines leaving the imidate moiety intact and instead undergoes straightforward CO→phosphine substitution (forming **6**), it was decided to perform some preliminary investigations upon the reactivity of the metal center in **3a**

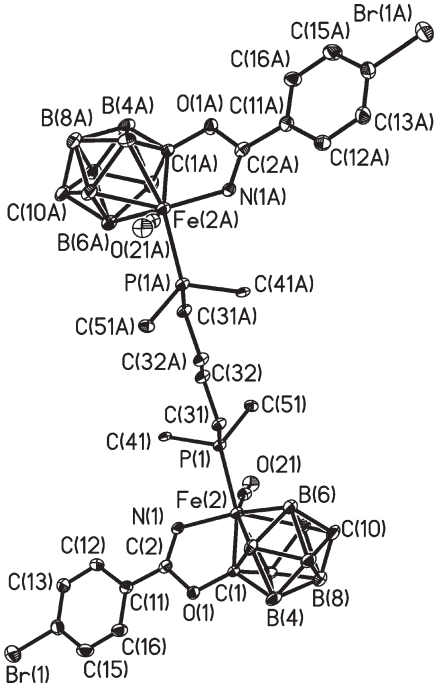

Figure 7. Structure of a whole molecule of **6** showing the crystallographic labeling scheme. For clarity only the *ipso*-C atoms of P-bound Ph rings are shown. Selected distances (Å) and angles (deg): C(1)−O(1) 1.426(5), C(1)−Fe(2) 1.926(4), O(1)−C(2) 1.347(5), C(2)−N(1) 1.284(5), N(1)−Fe(2) 1.962(4), Fe(2)−P(1) 2.2390(13); O(1)−C(1)−Fe(2) 117.2(3), C(2)−O(1)−C(1) 110.5(3), N(1)−C(2)−O(1) 116.1(4), C(2)−N(1)−Fe(2) 118.8(3), C(1)−Fe(2)−N(1) 77.01(16), C(1)−Fe(2)−P(1) 142.24(15), N(1)−Fe(2)−P(1) 92.56(11). Symmetry transformation, A: $1-x, -y, 1-z$.

toward donors, the latter being chosen as the simplest model for compounds of type **3**. Direct reaction with the phosphine $PHPh_2$, in the presence of Me_3NO, afforded as expected [2-CO-2-$PHPh_2$-1,2-μ-{OC(Me)NH}-*closo*-2,1,10-$FeC_2B_7H_8$] (**7**; see Scheme 2). In itself, compound **7** is relatively unremarkable, but it does further confirm the stability of the imidate moiety under Fe substitution. Its spectroscopic properties are as expected, and the structure was further confirmed by an X-ray diffraction study (included as Supporting Information).

The metal-bound phosphine ligand in the product **7** retains a reactive P−H bond as a site for potential further reaction, a feature that we have recently exploited in related systems.[12] Deprotonation of this {Fe−P*H*Ph_2} fragment in **7** is facile using a variety of bases; the resulting species, which contains an electron-rich phosphorus center, readily reacts with electrophiles or oxidizes in the presence of oxygen. Thus, for example, reaction of **7** with an excess of (wet) NEt_3 in CH_2Cl_2 solution yields after several days the anionic complex [2-CO-2-{P(O)Ph_2}-1,2-μ-{OC(Me)NH}-*closo*-2,1,10-$FeC_2B_7H_8]^-$, isolated as its $[NHEt_3]^+$ salt (**8**; Scheme 2). The conversion of the $PHPh_2$ ligand to a formal $\{P(O)Ph_2\}^-$ group was revealed by an X-ray diffraction experiment (see Figure 8) and is attributed to the presence of traces of H_2O in the NEt_3 reagent. As the figure shows, the P═O moiety is involved in hydrogen bonding with the N−H proton [H(2A)] of the cation; there is also a much weaker interaction with the imidate

Scheme 2. Formation of Compounds 7−11 from 3a[a]

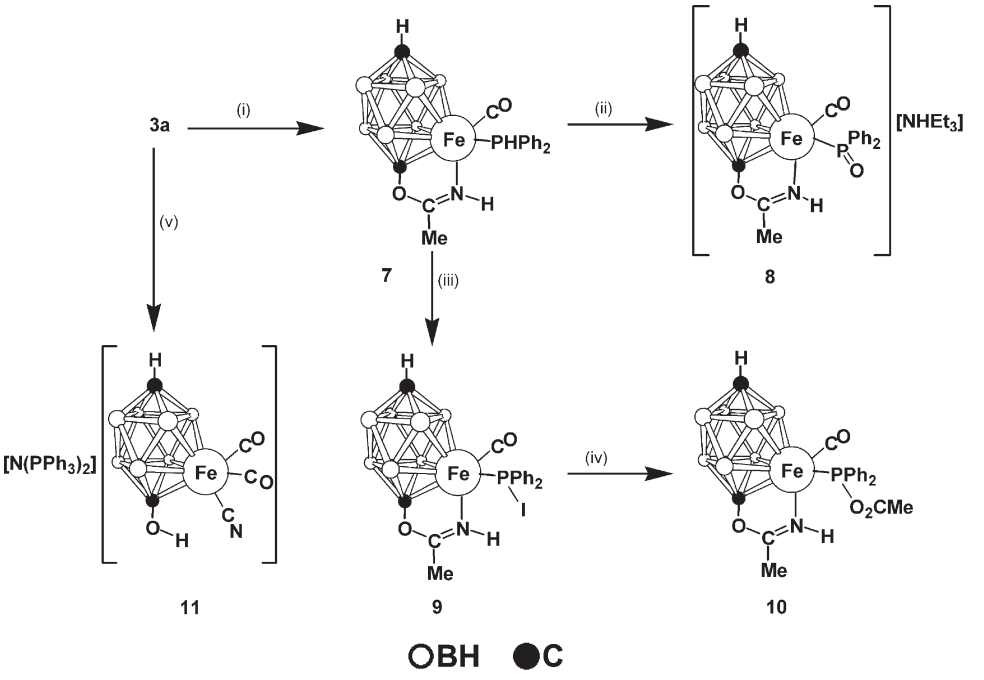

[a] Reagents and conditions: (i) $PHPh_2$−Me_3NO, CH_2Cl_2, 18 h; (ii) NEt_3−trace H_2O, CH_2Cl_2, 6 d; (iii) NEt_3−CH_2I_2, C_6H_6, 2 d; (iv) AgO_2CMe, CH_2Cl_2, 18 h; (v) excess $[NBu^n_4]CN$, CH_2Cl_2, 18 h; then $[N(PPh_3)_2]Cl$.

proton [H(1A)]. In the $^{31}P\{^1H\}$ NMR spectrum of **8**, the $\{P(O)Ph_2\}$ group gives rise to a low-field resonance at δ 157.6.[23,24]

When **7** was deprotonated with NEt_3 in a mixture of C_6H_6−CH_2I_2, in the hope of forming a dimeric product with a P−CH_2−P bridge via double nucleophilic substitution of the CH_2I_2 molecule, the product instead was found to be [2-CO-2-$PIPh_2$-1,2-μ-{OC(Me)NH}-*closo*-2,1,10-$FeC_2B_7H_8$] (**9**). Complex **9** was highly unexpected, but nevertheless its structure was confirmed unequivocally via a single-crystal X-ray diffraction experiment, the results of which are shown in Figure 9. The P−H unit of the precursor has clearly been replaced by P−I [P(1)−I(1) = 2.4777(15) Å], a fact corroborated by ^{31}P NMR spectroscopy. Thus, the ^1H-decoupled ^{31}P NMR spectrum shows a singlet resonance (δ 133.2) that retains this multiplicity in the corresponding proton-coupled spectrum. [The latter may be compared with δ_P 56.8 for compound **7**, with ^1J(HP) = 372 Hz.] Mechanistically it is far from clear how **7** is converted to **9** under these reaction conditions. However, we have confirmed that reaction of **7** in C_6H_6 with I_2 and NEt_3 affords no such product, essentially ruling out the possibility of a formal H^+/I^+ exchange.

Compound **9** can also itself be further derivatized by reaction with AgO_2CMe to eliminate AgI and produce the

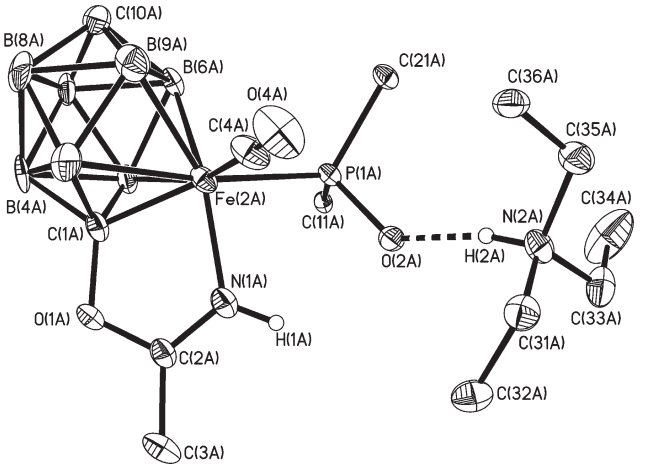

Figure 8. Structure of one of the crystallographically independent ion pairs of the salt **8** showing the crystallographic labeling scheme. For clarity only the *ipso*-C atoms of P-bound Ph rings are shown. Selected distances (Å) and angles (deg): C(1A)−O(1A) 1.440(7), C(1A)−Fe(2A) 1.921(6), O(1A)−C(2A) 1.332(7), C(2A)−N(1A) 1.266(7), N(1A)−Fe(2A) 1.958(5), Fe(2A)−P(1A) 2.2189(16), P(1A)−O(2A) 1.553(4), C(1A)−Fe(2A)−N(1A) 77.3(2), C(1A)−Fe(2A)−P(1A) 136.9(2), O(2A)−P(1A)−Fe(2A) 110.90(16), N(1A)−H(1A) 0.88, H(1A)···O(2A) 2.32, N(1A)···O(2A) 2.856(6), N(1A)−H(1A)···O(2A) 119.7, N(2A)−H(2A) 0.93, H(2A)···O(2A) 1.68, N(2A)···O(2A) 2.597(6), N(2A)−H(2A)···O(2A) 168.1.

P-acetato derivative [2-CO-2-{$P(O_2CMe)Ph_2$}-1,2-μ-{OC(Me)NH}-*closo*-2,1,10-$FeC_2B_7H_8$] (**10**). This compound shows some similarities to compound **9** (their ^{11}B NMR data parallel each other), but also to **8**, notably a very low-field $^{31}P\{^1H\}$ NMR resonance at δ 177.1. The direct phosphorus-to-acetate linkage was confirmed by an X-ray diffraction experiment (Figure 10), which additionally shows weak

(23) Kühl, O. *Phosphoros-31 NMR Spectroscopy*; Springer Verlag: Berlin, Germany, 2008.

(24) Compound **8** appeared to be somewhat unstable and tended to decompose into a variety of related species depending on conditions. Thus, although crystals of **8** as described here could be obtained by diffusion of petroleum ether into a CH_2Cl_2 solution, crystallization instead from CH_2Cl_2−Et_2O produced an Et_2O solvate of a neutral species where the phosphorus ligand was protonated, existing as $\{P(OH)Ph_2\}$. Likewise, crystals of a derivative of **8** where the appended phosphorus group instead was $\{PPh_2OP(=O)Ph_2\}$ were obtained surreptitiously, formation of this highly unusual diphosphorus ligand obviously requiring some decomposition of **8**. Details of both of these species' crystal structures, designated compounds **8a** and **8b**, respectively, are included as Supporting Information.

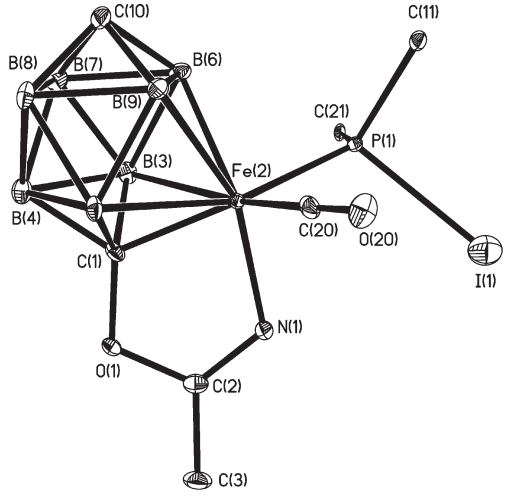

Figure 9. Structure of compound **9** showing the crystallographic labeling scheme. For clarity only the *ipso*-C atoms of P-bound Ph rings are shown. Selected distances (Å) and angles (deg): C(1)−O(1) 1.417(6), C(1)−Fe(2) 1.927(6), O(1)−C(2) 1.339(7), C(2)−N(1) 1.283(8), N(1)−Fe(2) 1.976(5), Fe(2)−P(1) 2.1797(16), P(1)−I(1) 2.4777(15); O(1)−C(1)−Fe(2) 116.7(4), C(2)−O(1)−C(1) 111.3(4), N(1)−C(2)−O(1) 116.6(5), C(2)−N(1)−Fe(2) 117.6(4), C(1)−Fe(2)−N(1) 77.2(2), C(1)−Fe(2)−P(1) 141.63(17), N(1)−Fe(2)−P(1) 94.75(15), Fe(2)−P(1)−I(1) 111.78(6).

*intra*molecular N−H···O=C(O)Me hydrogen bonding [the H···O and N···O distances are 2.55(2) and 3.0889(18) Å, respectively, with an N−H···O angle of 126.6(17)°] aided by the close spatial proximity of the {NH} and {O_2CMe} moieties, along with a similar *inter*molecular interaction [H···O = 2.55(2) Å, N···O = 3.0468(18) Å, N−H···O = 120.5(17)°]; this pair of interactions is repeated (across a crystallographic inversion center) so that overall four hydrogen bonds form a {H···O···H···O···} parallelogram.

In addition to substitution at Fe in **3a** by neutral donors, it was also of interest to replace a CO ligand with an anionic species, to give a charged product that might undergo further reaction with nucleophiles.[25] This was achieved by treatment of **3a** with [NBu^n_4]CN in CH_2Cl_2. However, the product was not the expected one, but instead was [1-OH-2,2-$(CO)_2$-2-CN-*closo*-2,1,10-$FeC_2B_7H_8$], in which the intramolecular imidate portion of the precursor has been lost. It was isolated as its $[N(PPh_3)_2]^+$ salt (**11**; see Scheme 1) following addition of $[N(PPh_3)_2]$Cl. (Attempts to prepare the anion of **11** directly by reaction between **1a** and [NBu^n_4]CN were unsuccessful, and it is not entirely clear how it is formed from **3a**.) This result is clearly also somewhat surprising given the known stability of five-membered rings and the demonstrated stability of compounds **3** discussed above. Conceivably, however, initial CO→CN^- substitution in **3a** gives an anionic species that is susceptible to proton attack, leading to hydrolysis of the imidate moiety. Spectroscopic data for compound **11** were useful in confirming the proposed architecture. In particular, ^{1}H and $^{13}C\{^1H\}$ NMR spectra showed no evidence of the imidate group, with instead two broad resonances [δ_H = 6.33 and 3.78] assignable[8] to the H atoms of cage {CH} and {COH} vertexes, respectively, and a signal at δ_C = 145.1 for the C≡N group.

In seeking to preparing a neutral derivative of compound **11**, reaction with an excess of the cationic iridium synthon

(25) Franken, A.; McGrath, T. D.; Stone, F. G. A. *Organometallics* **2008**, *27*, 148.

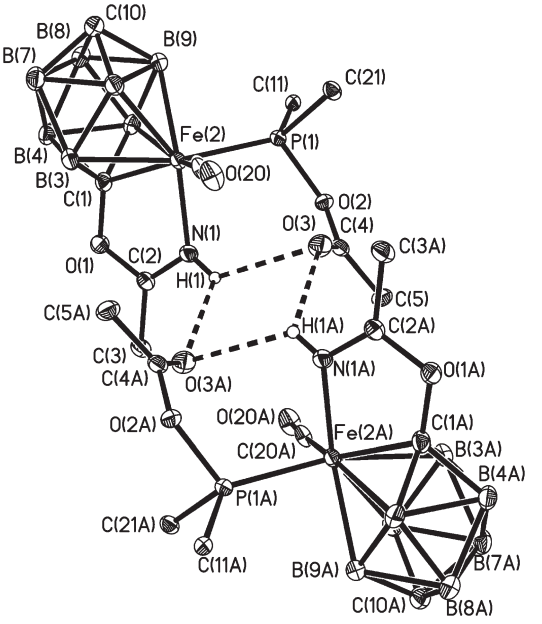

Figure 10. Hydrogen-bonded pair of molecules of compound **10** showing the crystallographic labeling scheme. For clarity only the *ipso*-C atoms of P-bound Ph rings and only the H atoms involved in hydrogen bonding are shown. Selected distances (Å) and angles (deg): C(1)−O(1) 1.4203(18), C(1)−Fe(2) 1.9235(15), O(1)−C(2) 1.3387(19), C(2)−N(1) 1.279(2), N(1)−Fe(2) 1.9733(14), Fe(2)−P(1) 2.1903(4), P(1)−O(2) 1.6877(11), O(2)−C(4) 1.3666(19), O(3)−C(4) 1.2012(19), N(1)−H(1) 0.79(2), N(1)···O(3) 3.0889(18), H(1)···O(3) 2.55(2), N(1)···O(3A) 3.0468(18), H(1)···O(3A) 2.57(2); N(1)−H(1)···O(3) 126.6(17), N(1)−H(1)···O(3A) 120.5(17). Symmetry transformation A: $-x$, $-1-y$, $-z$.

Chart 5

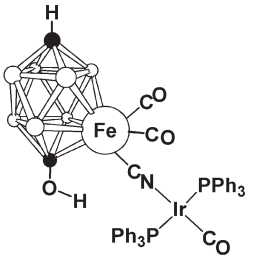

12

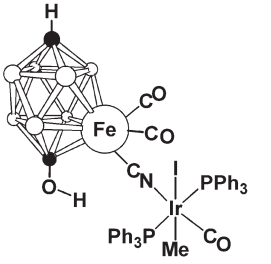

13

○BH ●C

$\{Ir(CO)(PPh_3)_2\}^+$, obtained from $[IrCl(CO)(PPh_3)_2]-TlPF_6$, afforded the bimetallic compound [2-{(μ-CN)Ir(CO)$(PPh_3)_2$}-2,2-$(CO)_2$-1-OH-*closo*-2,1,10-$FeC_2B_7H_8$] (**12**; see Chart 5).

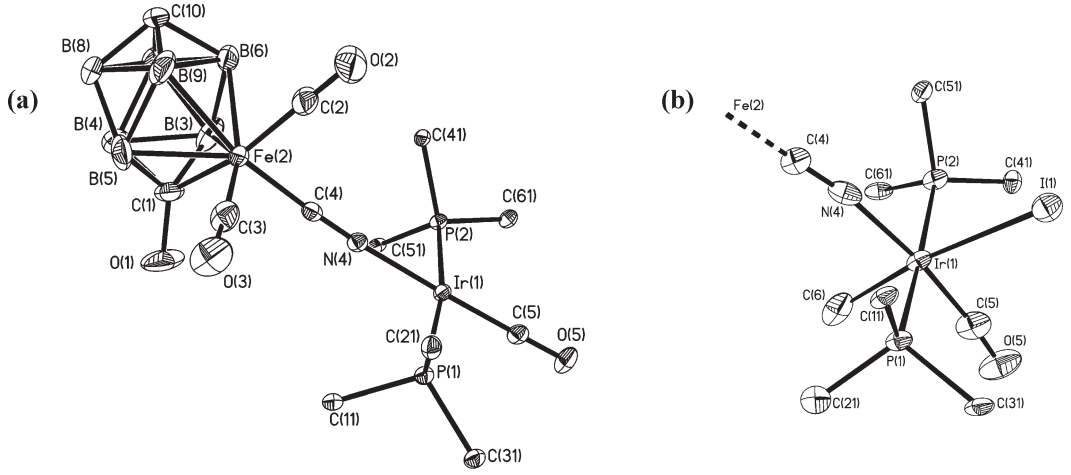

Figure 11. Structures of (a) compound **12** and (b) compound **13**, showing the crystallographic labeling schemes. For clarity only the *ipso*-C atoms of P-bound Ph rings are shown, and in (b) only the coordination geometry around iridium is shown. Selected distances (Å) and angles (deg): (a) Fe(2)−C(4) 1.895(3), C(4)−N(4) 1.154(4), N(4)−Ir(1) 2.056(3), Ir(1)−C(5) 1.825(3), Ir(1)−P(1) 2.3178(8), Ir(1)−P(2) 2.3310(8), N(4)−C(4)−Fe(2) 175.9(3), C(4)−N(4)−Ir(1) 173.2(2), C(5)−Ir(1)−N(4) 176.29(11), N(4)−Ir(1)−P(1) 86.35(7), N(4)−Ir(1)−P(2) 87.37(7), P(1)−Ir(1)−P(2) 169.05(3). (b) Fe(2)−C(4) 1.900(11), C(4)−N(4) 1.137(12), N(4)−Ir(1) 2.050(10), Ir(1)−C(5) 1.882(12), Ir(1)−C(6) 2.206(12), Ir(1)−I(1) 2.7998(9), Ir(1)−P(1) 2.378(2), Ir(1)−P(2) 2.390(2), N(4)−C(4)−Fe(2) 175.5(10), C(4)−N(4)−Ir(1) 171.3(8), C(5)−Ir(1)−N(4) 172.7(5), N(4)−Ir(1)−C(6) 89.0(4), N(4)−Ir(1)−P(1) 85.9(2), N(4)−Ir(1)−P(2) 88.1(2), C(6)−Ir(1)−P(1) 91.7(3), C(6)−Ir(1)−P(2) 92.7(3), P(1)−Ir(1)−P(2) 172.53(8), N(4)−Ir(1)−I(1) 99.5(2), C(6)−Ir(1)−I(1) 171.5(3), P(1)−Ir(1)−I(1) 89.17(7), P(2)−Ir(1)−I(1) 87.34(7).

An X-ray diffraction study definitively established the structure of **12**, depicted in Figure 11a. The iridium moiety is clearly appended in a site exopolyhedral to the $\{FeC_2B_7\}$ cluster, anchored to iron via a bridging cyanide group, with the carbonyl and cyanide ligands dictating a *trans* geometry about the iridium center as in the starting Vaska's compound. Like the latter, the square-planar iridium atom in compound **12** is a 16-electron (d^8) center and undergoes oxidative addition reactions with, for example, alkyl halides. Thus, treatment of CH_2Cl_2 solutions of **12** with MeI affords [2-{(μ-CN)Ir(I)(Me)(CO)-$(PPh_3)_2$}-2,2-$(CO)_2$-1-OH-*closo*-2,1,10-$FeC_2B_7H_8$] (**13**), containing an octahedral, 18-electron (d^6) iridium moiety, whose structure is represented in Figure 11b. In broad terms, the coordination environment around Ir is approximately similar to that in **12**, with the Me and I ligands adding above and below the plane, as expected.[26] Compared with **12**, however, there is significant lengthening of the iridium···(ligand) distances (ligand = CO, NC^-, PPh_3) upon formation of **13**: this has been observed previously[27] and may be attributed to diminished Ir→(ligand) back-bonding upon oxidation of the metal center. Not surprisingly, the structure of the $\{FeC_2B_7\}$ cluster, on the other hand, is essentially unaffected by the MeI addition at iridium.

Spectroscopic data for compounds **12** and **13** likewise show almost identical ferracarborane moieties—their $^{11}B\{^1H\}$ NMR spectra are almost superimposable—but distinctly different iridium centers. The Ir-bound PPh_3 ligands give rise to $^{31}P\{^1H\}$ NMR signals at δ 23.3 in **12**, but these resonances are shifted to lower field (δ −13.4) in **13** upon oxidation of the metal center, while the protons of the methyl group in **13** resonate at δ 1.60, with a corresponding peak at δ 15.3 in the $^{13}C\{^1H\}$ NMR spectrum.

Conclusions

The pendant cage−OH group in compounds such as **1a** has previously been shown[9,10] to serve as a point where different types of cluster functionalization can be achieved. In the present work we have extended and broadened this property, demonstrating that synergy between the hydroxyl group and the adjacent Fe center allows intramolecular attack upon a metal-bound ligand, yielding two different types of species possessing five-membered intramolecular rings (compounds **2** and **3**). Moreover, the fixed relative orientations of the nitrile and *C*(cage)−hydroxyl groups mean that the attack upon the coordinated nitrile is constrained to proceed with complete stereochemical control, affording exclusively the *Z* conformation of the resulting imino ester in compounds **3**.[16] With the ability to incorporate a range of substituents demonstrated for these compounds, along with the evident stability (as yet unoptimized) of the cluster−imidate linkage, opportunities clearly exist for incorporating these clusters into materials with useful applications: metallacarboranes have, for example, been successfully integrated into poly(pyrrole) materials with dramatic improvements to the polymer's properties.[3a] This is a target for which compounds **3** merit future evaluation.

In the present case we have turned in a different direction and have exploited the stability of compounds **3** to obtain larger, supramolecular species such as the bis(cluster) molecule **6** and the tetracluster, hexametallic complex **5**.[11] Hydrogen-bonding interactions similar to those observed in crystals of compounds **1** and **3** can also be exploited to engineer more elaborate, multimolecular assemblies.[28] Bimetallic compounds such as **4**, in which the two metal centers are linked via an extended conjugated system, are of considerable current interest[29] and

(26) For example: Labinger, J. A.; Osborn, J. A. *Inorg. Chem.* **1980**, *19*, 3230. Griffin, T. R.; Cook, D. B.; Haynes, A.; Pearson, J. M.; Monti, D.; Morris, G. E. *J. Am. Chem. Soc.* **1996**, *118*, 3029. Janka, M.; Atesin, A. C.; Fox, D. J.; Flaschenriem, C.; Brennessel, W. W.; Eisenberg, R. *Inorg. Chem.* **2006**, *45*, 6559.

(27) Cambridge Structural Database: Allen, F. H. *Acta Crystallogr.* **2002**, *B58*, 380.

(28) For example: Desiraju, G. R. *Acc. Chem. Res.* **2002**, *35*, 565.

(29) For example: (a) Astruc, D. *Acc. Chem. Res.* **1997**, *30*, 383. (b) Ceccon, A.; Santi, S.; Orian, L.; Bisello, A. *Coord. Chem. Rev.* **2004**, *248*, 683. (c) Xi, B.; Xu, G.-L.; Fanwick, P. E.; Ren, T. *Organometallics* **2009**, *28*, 2338.

is an area where we plan to invest future effort. Likewise, two metal centers in close proximity can operate cooperatively in (for example) catalysis: compounds **12** and **13**, and the ease with which the former readily undergoes oxidative addition (to yield the latter), may be relevant to such systems.[30] In a subsequent paper,[31] we shall report the synthesis and selected reactivity of carboxylate $\overline{\text{FeOCOC}}$ analogues of compounds **3**, along with C_{cage}−phosphorus-containing derivatives. These species further illustrate the diversity possible in this $\{FeC_2B_7\}$ system and which we hope will herald yet other classes of product that will become accessible with the development of these synthetic protocols.

Experimental Section

General Considerations. All reactions were carried out under an atmosphere of dry nitrogen using standard Schlenk line techniques. Solvents were stored over and distilled from appropriate drying agents under nitrogen prior to use. Petroleum ether refers to that fraction of boiling point 40−60 °C. Chromatography columns (typically ca. 20 cm in length and ca. 2 cm in diameter) were packed with silica gel (Acros, 60−200 mesh). Elemental analyses were performed by Atlantic Microlab, Inc., Norcross, GA, upon crystalline or microcrystalline samples that had been dried overnight in vacuo. On occasion residual solvent remained after drying, its presence and approximate proportion confirmed by integrated ^{1}H NMR spectroscopy, and this was factored into the calculated microanalysis data. IR spectra were recorded from CH_2Cl_2 solutions. NMR spectra were recorded at the following frequencies (MHz): ^{1}H, 360.13; ^{13}C, 90.56; ^{11}B, 115.5; and ^{31}P, 145.78. Proton-decoupled ^{31}P chemical shifts (δ) are quoted in ppm with positive numbers to high frequency of 85% H_3PO_4 (external). Compound **1a** was synthesized following the literature procedure.[9]

Synthesis of [2,2-(CO)$_2$-1,2-μ-{OCH$_2$NMe$_2$}-*closo*-2,1,10-FeC$_2$B$_7$H$_8$] (2). Compound **1a** (0.13 g, 0.49 mmol), dissolved in CH_2Cl_2 (20 mL), was treated with Me_3NO (0.08 g, 1.1 mmol) and the mixture stirred at ambient temperature for 18 h. Volatiles were removed under reduced pressure, and the residue was dissolved in CH_2Cl_2−petroleum ether (3:2, 5 mL) and transferred to the top of a chromatography column. Elution with the same solvent mixture gave a yellow fraction; removal of solvents from the latter yielded yellow microcrystals of **2** (0.06 g, 43%). Anal. Found: 28.2% C, 5.4% H, 4.6% N. Calcd: 28.6% C, 5.5% H, 4.8% N. IR: ν_{max}(CO) 2029 s, 1983 s cm^{-1}.

Synthesis of [2,2-(CO)$_2$-1,2-μ-{OC(R)NH}-*closo*-2,1,10-FeC$_2$B$_7$H$_8$] [R = Me (3a), CH=C(H)Me (3c), *p*-C$_6$H$_4$NO$_2$ (3d), *p*-C$_6$H$_4$NH$_2$ (3e), *p*-C$_6$H$_4$Br (3f), *p*-C$_6$H$_4$C(H)O (3g), *p*-C$_6$H$_4$-C≡CH (3h), *p*-C$_5$H$_4$N (3i), NH$_2$ (3j)]. (i) Compound **1a** (0.13 g, 0.49 mmol) was dissolved in CH_3CN (20 mL), Me_3NO (0.08 g, 1.1 mmol) was added, and the mixture was stirred at ambient temperature for 18 h. Solvent was removed under reduced pressure, and the residue was dissolved in CH_2Cl_2−petroleum ether (1:1, 5 mL) and transferred to the top of a chromatography column. Eluting with the same mixture gave an orange fraction, removal of solvents from which yielded orange microcrystals of **3a** (0.09 g, 63%). Anal. Found: 26.0% C, 4.5% H, 5.0% N. Calcd: 26.0% C, 4.4% H, 5.0% N. IR: ν_{max}(CO) 2039 s, 1993 s cm^{-1}.

(ii) By an analogous procedure, compound **1a** (0.13 g, 0.49 mmol) with CH_2=CHCH$_2$CN (0.4 mL, 5 mmol) and Me_3NO (0.08 g, 1.1 mmol) in CH_2Cl_2 (20 mL), and using CH_2Cl_2−petroleum ether (2:3) as chromatographic eluant, gave orange microcrystals of **3c** (0.10 g, 63%). Anal. Found: 31.6% C, 4.7% H, 4.6% N. Calcd: 31.6% C, 4.7% H, 4.6% N. IR: ν_{max}(CO) 2040 s, 1996 s cm^{-1}.

(iii) Similarly, compound **1a** (0.13 g, 0.49 mmol), *p*-(O$_2$N)-C$_6$H$_4$CN (0.15 g, 1.0 mmol), and Me_3NO (0.08 g, 1.1 mmol) in CH_2Cl_2 (20 mL), and using CH_2Cl_2−petroleum ether (3:2) as chromatographic eluant, gave orange microcrystals of **3d** (0.10 g, 51%). Anal. Found: 34.2% C, 3.3% H, 7.1% N. Calcd: 34.3% C, 3.4% H, 7.3% N. IR: ν_{max}(CO) 2043 s, 1999 s cm^{-1}; ν_{max}-(NO) 1533 m, 1348 m cm^{-1}.

(iv) Compound **3d** (0.10 g, 0.26 mmol) was dissolved in EtOH (10 mL), $NaBH_4$ (0.040 g, 1.1 mmol) was added, and the mixture was stirred at ambient temperature for 30 min. Solvent was removed under reduced pressure, and the residue extracted into neat CH_2Cl_2 and transferred on top of a chromatography column. Eluting with the same solvent gave an orange fraction, removal of solvents from which afforded orange microcrystals of **3e** (0.040 g, 42%). Anal. Found: 37.0% C, 4.4% H, 7.7% N. Calcd: 37.2% C, 4.3% H, 7.9% N. IR: ν_{max}(CO) 2038 s, 1994 s cm^{-1}.

(v) Similar to the synthesis of **3d**, compound **1a** (0.13 g, 0.49 mmol), *p*-BrC$_6$H$_4$CN (0.36 g, 2.0 mmol), and Me_3NO (0.08 g, 1.1 mmol) in CH_2Cl_2 (20 mL), and using CH_2Cl_2−petroleum ether (1:1) as chromatographic eluant, gave orange microcrystals of **3f** (0.15 g, 71%). Anal. Found: 31.5% C, 3.0% H, 3.2% N. Calcd: 31.6% C, 3.1% H, 3.4% N. IR: ν_{max}(CO) 2041 s, 1997 s cm^{-1}.

(vi) Similar to the synthesis of **3d**, compound **1a** (0.13 g, 0.49 mmol), *p*-OC(H)C$_6$H$_4$CN (0.26 g, 2.0 mmol), and Me_3NO (0.08 g, 1.1 mmol) in CH_2Cl_2 (20 mL), and using CH_2Cl_2−petroleum ether (4:1) as chromatographic eluant, gave orange microcrystals of **3g** (0.10 g, 54%). Anal. Found: 39.2% C, 3.7% H, 3.7% N. Calcd: 39.2% C, 3.8% H, 3.8% N. IR: ν_{max}(C≡O) 2043 s, 2000 s cm^{-1}; ν_{max}(C=O) 1709 m cm^{-1}.

(vii) Similar to the synthesis of **3d**, compound **1a** (0.13 g, 0.49 mmol), *p*-(HC≡C)C$_6$H$_4$CN (0.26 g, 2.0 mmol), and Me_3NO (0.08 g, 1.1 mmol) in CH_2Cl_2 (20 mL) gave orange microcrystals of **3h** (0.13 g, 72%). Anal. Found: 41.4% C, 3.9% H, 3.7% N. Calcd: for **3h**·0.25CH_2Cl_2 41.3% C, 3.8% H, 3.6% N. IR: ν_{max}(CO) 2041 s, 1997 s cm^{-1}.

(viii) Similar to the synthesis of **3d**, compound **1a** (0.13 g, 0.49 mmol) was treated with *p*-NC-C$_5$H$_4$N (0.20 g, 1.9 mmol) and Me_3NO (0.08 g, 1.1 mmol) in CH_2Cl_2 (20 mL). The evaporated reaction mixture was extracted with CH_2Cl_2, and CH_2Cl_2−THF (48:2) was used as chromatographic eluant, giving orange microcrystals of **3i** (0.11 g, 67%). Anal. Found: 35.2% C, 3.9% H, 8.1% N. Calcd: 35.3% C, 3.9% H, 8.2% N. IR: ν_{max}(CO) 2043 s, 2000 s cm^{-1}.

(ix) Similar to the synthesis of **3i**, compound **1a** (0.13 g, 0.49 mmol) was dissolved in CH_2Cl_2 (15 mL) and treated overnight with NH_2CN (0.100 g, 2.4 mmol) and Me_3NO (0.05 g, 0.66 mmol). Using CH_2Cl_2 as the chromatographic mobile phase gave red microcrystals of **3j** (0.091 g, 67%). Anal. Found: 22.0% C, 4.0% H, 10.1% N. Calcd: 21.6% C, 4.0% H, 10.1% N. IR: ν_{max}(CO) 2038 s, 1992 s cm^{-1}.

Synthesis of [2,2-(CO)$_2$-*closo*-2,1,10-FeC$_2$B$_7$H$_8$-1,2-μ-{OC-(N^{Fe}H)-*p*-C$_6$H$_4$-C≡C}]$_2$ (4). Compound **3h** (0.13 g, 0.35 mmol) was dissolved in CH_2Cl_2 (20 mL), [CuCl(TMEDA)] (0.13 g, 0.60 mmol) was added, and air was passed through the stirred suspension for 3 h. Volatiles were removed under reduced pressure, and the residue was dissolved in CH_2Cl_2−petroleum ether (3:2, 5 mL) and applied to a chromatography column. Eluting with CH_2Cl_2−petroleum ether (1:1) gave an orange fraction, removal of solvents from which yielded orange microcrystals of **4** (0.10 g, 82%). Anal. Found: 42.1% C, 3.5% H, 3.8% N. Calcd: for **4**·0.25CH_2Cl_2 42.2% C, 3.6% H, 3.8% N. IR: ν_{max}(CO) 2041 s, 1997 s cm^{-1}.

(30) See, for example: (a) Motta, A.; Fragala, I. L.; Marks, T. J. *J. Am. Chem. Soc.* **2009**, *131*, 3974. (b) Martin, M.; Sola, E.; Tejero, S.; Lopez, J. A.; Oro, L. A. *Chem.−Eur. J.* **2006**, *12*, 4057. (c) Molenveld, P.; Engbersen, J. F. J.; Reinhoudt, D. N. *Chem. Soc. Rev.* **2000**, *29*, 75. (d) Matsunaga, S.; Ohshima, T.; Shibasaki, M. *Adv. Synth. Catal.* **2002**, *344*, 3, and references therein.

(31) Franken, A.; McGrath, T. D.; Stone, F. G. A. *Organometallics*, in preparation.

Table 2. Data for Crystal Structure Analyses

	1a	**1a**·0.5H_2O	**2**	**3d**
formula	$C_5H_9B_7FeO_4$	$C_5H_{10}B_7FeO_{4.5}$	$C_7H_{16}B_7FeNO_3$	$C_{11}H_{13}B_7FeN_2O_5$
fw	264.64	273.65	293.73	384.75
space group	$P\bar{1}$	$P4_2/n$	$P2_1/n$	$P2_1/n$
a, Å	7.4943(4)	18.0816(11)	7.913(2)	7.1973(2)
b, Å	11.5596(6)	18.0816(11)	14.313(4)	14.6216(5)
c, Å	19.5362(10)	7.3449(7)	11.945(3)	16.3759(6)
α, deg	93.420(2)	90	90	90
β, deg	97.911(2)	90	101.863(5)	99.126(2)
γ, deg	90.151(2)	90	90	90
V, Å^3	1673.25(15)	2401.4(3)	1324.0(6)	1701.52(10)
Z	6	8	4	4
μ (Mo Kα), cm^{-1}	1.337	1.248	1.131	0.910
reflns measd	22 463	19 098	12 753	12 424
indept reflns	6260	3070	3474	3384
R_{int}	0.0555	0.0601	0.0507	0.0579
wR_2, R_1 (all data)[a]	0.0843, 0.0594	0.0903, 0.0624	0.0905, 0.0633	0.0916, 0.0609
	3g	**3i**	**6**	**8**
formula	$C_{12}H_{14}B_7FeNO_4$	$C_{10}H_{13}B_7FeN_2O_3$	$C_{48}H_{54}B_{14}Br_2Fe_2N_2O_4P_2$	$C_{23}H_{38}B_7FeN_2O_3P$
fw	367.76	340.74	1207.73	553.04
space group	$P2_1/c$	$R\bar{3}$	$P\bar{1}$	$P2_1/c$
a, Å	8.3973(5)	27.730(2)	10.6153(17)	19.510(2)
b, Å	12.6216(7)	27.730(2)	11.1988(18)	9.6131(12)
c, Å	31.446(2)	11.6194(7)	12.078(2)	30.723(4)
α, deg	90	90	69.099(9)	90
β, deg	100.023(2)	90	80.012(10)	99.041(3)
γ, deg	90	120	84.448(10)	90
V, Å^3	3282.0(3)	7737.7(9)	1320.1(4)	5690.7(12)
Z	8	18	1	8
μ (Mo Kα), cm^{-1}	0.934	0.883	2.170	0.614
reflns measd	45 850	30 774	21 523	49 799
indept reflns	6005	3160	4751	10 324
R_{int}	0.0469	0.0543	0.0925	0.0918
wR_2, R_1 (all data)[a]	0.0796, 0.0385	0.0979, 0.0531	0.1109, 0.1024	0.2063, 0.1276
	9	**10**	**12**	**13**
formula	$C_{17}H_{22}B_7FeINO_2P$	$C_{19}H_{25}B_7FeNO_4P$	$C_{42}H_{39}B_7FeIrNO_4P_2$	$C_{47}H_{52}B_7FeIIrNO_5P_2$
fw	561.75	493.89	1007.40	1223.46
space group	$P\bar{1}$	$C2/c$	$P\bar{1}$	$P\bar{1}$
a, Å	9.0292(4)	39.2433(10)	11.0443(12)	12.0508(8)
b, Å	10.2857(5)	7.4402(2)	11.9579(13)	12.6131(8)
c, Å	13.4485(7)	20.8096(8)	16.7449(18)	18.9809(14)
α, deg	92.818(3)	90	80.322(6)	74.222(5)
β, deg	103.850(2)	121.487(2)	82.072(6)	82.021(5)
γ, deg	111.942(2)	90	81.824(6)	63.881(4)
V, Å^3	1111.42(9)	5181.3(3)	2143.0(4)	2492.2(3)
Z	2	8	2	2
μ (Mo Kα), cm^{-1}	2.154	0.669	3.557	3.687
reflns measd	33 458	44 765	37 046	30 314
indept reflns	5337	6654	14 416	8636
R_{int}	0.0354	0.0513	0.0465	0.0862
wR_2, R_1 (all data)[a]	0.1729, 0.0756	0.0918, 0.0429	0.0744, 0.0551	0.1297, 0.0939

[a] $wR_2 = [\sum\{w(F_o^2 - F_c^2)^2\}/\sum w(F_o^2)^2]^{1/2}$; $R_1 = \sum||F_o| - |F_c||/\sum|F_o|$.

Synthesis of [2,2-(CO)$_2$-*closo*-2,1,10-FeC$_2$B$_7$H$_8$-1,2-*μ*-{OC(N^{Fc}H)-*p*-C$_6$H$_4$-{(*μ*-*η*^{2}:*η*^{2}-C≡C)Co$_2$(CO)$_6$}}]$_2$ (5). Compound **4** (0.09 g, 0.13 mmol) was dissolved in CH_2Cl_2 (20 mL), [$Co_2(CO)_8$] (0.17 g, 0.5 mmol) was added, and the mixture was stirred at ambient temperature for 18 h. Volatiles were removed under reduced pressure, and the residue was dissolved in CH_2Cl_2−petroleum ether (3:2, 5 mL) and subjected to column chromatography. Eluting with petroleum ether yielded a yellow-brown band identified (IR) as [$Co_2(CO)_8$], which was discarded. Thereafter, elution with CH_2Cl_2−petroleum ether (1:1) gave another yellow-brown fraction, from which were obtained red microcrystals of **5** (0.15 g, 87%) after evaporation in vacuo. Anal. Found: 35.0% C, 1.9% H, 2.2% N. Calcd: 35.2% C, 2.0% H, 2.2% N. IR: ν_{max}(CO) 2104 m, 2085 s, 2056 s, 2040 s, 1997 w cm^{-1}.

Synthesis of [2,2′-dppb-{2-CO-1,2-*μ*-{OC(C$_6$H$_4$Br)NH}-*closo*-2,1,10-FeC$_2$B$_7$H$_8$}$_2$] (6). Compound **3f** (0.15 g, 0.36 mmol) was dissolved in THF (20 mL), dppb (0.077 g, 0.18 mmol) was added, and the mixture was heated under reflux for 48 h. Solvent was removed under reduced pressure, and the residue was dissolved in CH_2Cl_2−petroleum ether (3:2, 5 mL) and chromatographed. Elution with CH_2Cl_2−petroleum ether (1:1) gave an orange fraction, removal of solvents from which yielded orange microcrystals of **6** (0.12 g, 57%). Anal. Found: 47.5% C, 4.3% H, 2.3% N. Calcd: 47.7% C, 4.5% H, 2.3% . IR: ν_{max}(CO) 1953 s cm^{-1}. ^{31}P NMR: *δ* 64.7.

Synthesis of [2-CO-2-PHPh$_2$-1,2-*μ*-{OC(Me)NH}-*closo*-2,1,10-FeC$_2$B$_7$H$_8$] (7). To a solution of **3a** (0.070 g, 0.25 mmol) in CH_2Cl_2 (20 mL) were added $PHPh_2$ (0.17 mL, 1.0 mmol) and Me_3NO (0.08 g, 1.1 mmol), and the resulting mixture was stirred at ambient temperature for 18 h. Volatiles were removed under reduced pressure, and the residue was dissolved in CH_2Cl_2−petroleum ether (1:1, 5 mL) and transferred on a chromatography column. Elution with the same mixture gave a red fraction, removal of solvents from which yielded red microcrystals of **7** (0.09 g, 82%). Anal. Found: 47.1% C, 5.5% H,

3.0% N. Calcd: 46.9% C, 5.3% H, 3.2% N. IR: ν_{max}(CO) 1955 s cm^{-1}. ^{31}P NMR: δ 56.8 [^{1}J(HP) = 372 Hz].

Synthesis of [NHEt$_3$][2-CO-2-{P(O)Ph$_2$}-1,2-μ-{OC(Me)-NH}-*closo*-2,1,10-FeC$_2$B$_7$H$_8$] (8). Compound **7** (0.11 g, 0.25 mmol) was dissolved in CH_2Cl_2 (20 mL), NEt_3 (1.0 mL, 7.2 mmol) was added, and the mixture was stirred at ambient temperature for 6 d. Volatiles were removed under reduced pressure, and the residue was dissolved in CH_2Cl_2 (5 mL) and chromatographed. Elution with CH_2Cl_2−THF (4:1) gave a red fraction, which yielded red microcrystals of **8** (0.07 g, 53%) upon evaporation in vacuo. Anal. Found: 49.9% C, 6.8% H, 5.0% N. Calcd: 50.0% C, 6.9% H, 5.1% N. IR: ν_{max}(CO) 1958 s cm^{-1}. ^{31}P NMR: δ 157.6.

Synthesis of [2-CO-2-PIPh$_2$-1,2-μ-{OC(Me)NH}-*closo*-2,1,10-FeC$_2$B$_7$H$_8$] (9). Compound **7** (0.11 g, 0.25 mmol) was dissolved in C_6H_6 (20 mL), CH_2I_2 (0.50 mL, 6.2 mmol) and NEt_3 (1.0 mL, 7.2 mmol) were added, and the resultant was stirred at ambient temperature for 2 d. After evaporation under reduced pressure, the residue was dissolved in CH_2Cl_2−petroleum ether (1:1, 5 mL) and chromatographed. Eluting with the same solvent mixture gave a red fraction. Removal of solvents from the latter yielded red microcrystals of **9** (0.07 g, 42%). Anal. Found: 36.2% C, 4.2% H, 2.6% N. Calcd: for **9** 36.4% C, 4.0% H, 2.5% N. IR: ν_{max}(CO) 1973 s cm^{-1}. ^{31}P NMR: δ 133.2.

Synthesis of [2-CO-2-{P(O$_2$CMe)Ph$_2$}-1,2-μ-{OC(Me)NH}-*closo*-2,1,10-FeC$_2$B$_7$H$_8$] (10). To a solution of **9** (0.14 g, 0.25 mmol) in CH_2Cl_2 (20 mL) was added AgO_2CMe (0.080 g, 0.48 mmol) and the mixture stirred at ambient temperature for 18 h. Workup as for **9** above yielded red microcrystals of **10** (0.08 g, 67%). Anal. Found: 46.3% C, 5.0% H, 2.6% N. Calcd: 46.2% C, 5.1% H, 2.8% N. IR: ν_{max}(C≡O) 1971 s cm^{-1}; ν_{max}(C═O) 1734 w cm^{-1}. ^{31}P NMR: δ 177.1.

Synthesis and Reactions of [N(PPh$_3$)$_2$][1-OH-2,2-(CO)$_2$-2-CN-*closo*-2,1,10-FeC$_2$B$_7$H$_8$] (11). (i) Compound **3a** (0.14 g, 0.50 mmol) and [NBu$^n_4$]CN (0.27 g, 1.0 mmol) were dissolved in CH_2Cl_2 (20 mL), and the solution was stirred at ambient temperature for 18 h. After addition of [N(PPh$_3$)$_2$]Cl (0.57 g, 1.0 mmol) and evaporation under reduced pressure, the remaining residue was dissolved in CH_2Cl_2 (5 mL) and transferred to the top of a chromatography column. Elution with CH_2Cl_2−THF (4:1) gave a yellow fraction, removal of solvents from which afforded yellow microcrystals of **11** (0.21 g, 52%). Anal. Found: 61.4% C, 4.7% H, 3.5% N. Calcd: 61.5% C, 4.9% H, 3.5% N. IR: ν_{max}(C≡N) 2101 w cm^{-1}; ν_{max}(C≡O) 2024 s, 1975 s cm^{-1}. ^{31}P NMR: δ 21.7.

(ii) A mixture of compound **11** (0.20 g, 0.25 mmol), [IrCl(CO)(PPh$_3$)$_2$] (0.20 g, 0.25 mmol), and TlPF$_6$ (0.090 g, 0.25 mmol) in CH_2Cl_2 (20 mL) was stirred at ambient temperature for 18 h. Volatiles were removed under reduced pressure, and the residue was extracted into CH_2Cl_2−petroleum ether (3:2, 3 mL) and applied to a chromatography column. Eluting with the same mixture of gave a yellow fraction, which, upon evaporation, yielded yellow microcrystals of [2-{(μ-CN)Ir(CO)(PPh$_3$)$_2$}-1-OH-2,2-(CO)$_2$-*closo*-2,1,10-FeC$_2$B$_7$H$_8$] (**12**) (0.18 g, 72%). Anal. Found: 49.9% C, 3.9% H, 1.3% N. Calcd: 50.1% C, 3.9% H, 1.4% N. IR: ν_{max}(C≡N) 2127 w cm^{-1}; ν_{max}(C≡O) 2033 s, 1988 s cm^{-1}. ^{31}P NMR: δ 23.3.

(iii) To compound **12** (0.20 g, 0.20 mmol) in CH_2Cl_2 (20 mL) was added MeI (30 μL, 0.5 mmol), and the mixture was stirred at ambient temperature for 18 h and then evaporated to dryness. The residue was dissolved in CH_2Cl_2−petroleum ether (1:1, 3 mL) and chromatographed. Elution with the same solvent mixture afforded a yellow fraction that yielded yellow microcrystals of [2-{(μ-CN)Ir(I)(Me)(CO)(PPh$_3$)$_2$}-1-OH-2,2-(CO)$_2$-*closo*-2,1,10-FeC$_2$B$_7$H$_8$] (**13**) (0.15 g, 67%). Anal. Found: 45.0% C, 3.6% H, 1.1% N. Calcd: 44.9% C, 3.7% H, 1.2% N. IR: ν_{max}(C≡N) 2137 w cm^{-1}; ν_{max}(C≡O) 2064 s, 2032 s, 2003 s cm^{-1}. ^{31}P NMR: δ −13.4.

X-ray Diffraction Experiments. Experimental data for all compounds studied are included as Supporting Information. Diffraction data were acquired[32] at 110(2) K using a Bruker-Nonius X8 Apex area-detector diffractometer (graphite-monochromated Mo Kα X-radiation, λ = 0.71073 Å). Several sets of data frames were collected at different θ values for various initial values of ϕ and ω, each frame covering a 0.5° increment of ϕ or ω. The data frames were integrated using SAINT.[32] The substantial redundancy in data allowed empirical absorption corrections (SADABS)[32] to be applied on the basis of multiple measurements of equivalent reflections.

All structures were solved using conventional direct methods[32−34] and refined by full-matrix least-squares on all F^2 data using SHELXTL version 6.12,[33,34] with anisotropic thermal parameters assigned to all non-H atoms. The locations of the cage-carbon atoms were verified by examination of the appropriate internuclear distances and the magnitudes of their isotropic thermal displacement parameters. All aryl, alkyl, and cluster H atoms were set riding in calculated positions, while attempts were made to allow reasonable positional refinement of N−H and O−H hydrogen atoms; where the latter could not be achieved, these hydrogens were likewise refined in riding or "rotating group"[33] positions. All H atoms had fixed isotropic thermal parameters defined as U_{iso}(H) = 1.2U_{iso}(parent), or U_{iso}(H) = 1.5U_{iso}(parent) for methyl groups.

Acknowledgment. We thank the Robert A. Welch Foundation (Grant AA-0006) and Baylor University for support, and Professor A. H. Cowley (University of Texas, Austin) for helpful discussions regarding the formation of compound **9**.

Supporting Information Available: Full details of the crystal structure analyses in CIF format (including those for compounds **3c**, **3f**, **3j**, **7**, **8a**, and **8b**); this material is available free of charge via the Internet at http://pubs.acs.org.

(32) *APEX 2*, version 1.0; Bruker AXS: Madison, WI, 2003−2004.
(33) Sheldrick, G. M. *Acta Crystallogr*. **2008**, *A64*, 112.
(34) *SHELXTL*, version 6.12; Bruker AXS: Madison, WI, 2001.